Distributed Binary Detection Over Fading Channels: Cooperative and Parallel Architectures

Nahal Maleki, *Student Member, IEEE*, Azadeh Vosoughi, *Senior Member, IEEE*, and Nazanin Rahnavard, *Member, IEEE*

***Abstract*—This paper considers the problem of binary distributed detection of a known signal in correlated Gaussian sensing noise in a wireless sensor network, where sensors are restricted to using the likelihood ratio test (LRT) and communicating with the fusion center (FC) over bandwidth-constrained channels that are subject to fading and noise. To mitigate the deteriorating effect of fading encountered in the conventional parallel fusion architecture, in which sensors directly communicate with the FC, we propose new fusion architectures that enhance the detection performance, via harvesting cooperative gain (so-called "decision diversity gain"). In particular, we propose 1) cooperative fusion architecture with Alamouti's space–time coding scheme at sensors, 2) cooperative fusion architecture with signal fusion at sensors, and 3) parallel fusion architecture with local threshold changing at sensors. For these schemes, we derive the LRT and majority fusion rules at the FC and provide upper bounds on the average error probabilities for homogeneous sensors, subject to uncorrelated Gaussian sensing noise, in terms of signal-to-noise ratio (SNR) of communication and sensing channels. Our simulation results indicate that when the FC employs the LRT rule, except for low communication SNR and moderate/high sensing SNR, performance improvement is feasible with the new fusion architectures. When the FC utilizes the majority rule, such an improvement is possible, except for high sensing SNR.**

***Index Terms*—Correlation, distributed detection, diversity, error floor, fusion and sensor rule, parallel architecture, space–time coding.**

I. Introduction

THE problem of distributed detection with the fusion center (FC; so-called classical parallel fusion architecture) has a long and rich history, where each local detector (sensor) processes its observation locally and independently and passes its local binary decision to the FC. The main assumption in the classical works is that the bandwidth-constrained communication channels are *error free*, and thus, the reliability of the final decision at the FC is determined by the reliability of the local binary decisions. However, wireless channels are inherently error prone, due to noise and fading. An *integrated approach* of distributed detection over noisy fading channels was considered in [1]–[12], in which the sensors send their modulated local binary decisions to the FC, and the FC employs a fusion rule, incorporating channel state information (CSI), to improve the reliability of the final decision at the FC. The performance of this integrated distributed detection is ultimately limited by the communication bounds. A common thread in the schemes discussed in [1]–[12] is that they are noncooperative, i.e., there is no information exchange among the sensors. Cooperative wireless communication [13], [18] has been proven to significantly enhance performance in the presence of fading, via invoking spatial diversity, that leads to the mitigation of the detrimental fading effects [13], [18]. Motivated by the promises of cooperative communication, we propose a new class of integrated distributed detection, which harvests cooperative gain (enabled by, at most, 1-bit information exchange among one-hop neighboring nodes) and improves the performance of the integrated distributed detection [1], [2] in the presence of fading, via allowing each sensor to send (at most) two information bits to the FC and assuming identical transmit power per node. In particular, we propose three schemes: 1) cooperative fusion architecture with Alamouti's space–time coding (STC) scheme at sensors, in which neighboring sensors exchange one information bit, and each sensor sends two information bits to the FC; 2) cooperative fusion architecture with signal fusion at sensors, in which neighboring sensors exchange one information bit, and each sensor sends one information bit to the FC; and 3) parallel fusion architecture with local threshold changing at sensors, in which neighboring sensors do not exchange information, and each sensor sends two information bits to the FC. To describe the proposed schemes, suppose $\mathcal{S}_1$ and $\mathcal{S}_2$ are two designated cooperative partners. *In scheme 1)*, rather than transmitting their local decisions directly to the FC, $\mathcal{S}_1$ and $\mathcal{S}_2$ are coordinated to form a transmit cluster, such that they first exchange their local decisions and apply Alamouti's scheme [19], [20] for transmitting the decisions to the FC. Different from most literature on distributed STC, which assume that a node acts as a relay only for error-free reception [21], we consider the fact that the channels between $\mathcal{S}_1$ and $\mathcal{S}_2$ are subject to errors, due to noise and fading. *In scheme 2)*, similar to scheme 1), $\mathcal{S}_1$ and $\mathcal{S}_2$ exchange their local decisions. Instead of applying Alamouti's scheme, however, each node updates its decision, via optimally fusing its observation with the received signal from its cooperative partner. Updated decisions are transmitted

Manuscript received March 6, 2014; revised September 18, 2014, May 28, 2015, and September 2, 2015; accepted October 4, 2015. Date of publication November 2, 2015; date of current version September 15, 2016. This paper was presented in part at the 10th IEEE International Workshop on Signal Processing Advances in Wireless Communications, Perugia, Italy, June 21–24, 2009. This work was supported by the National Science Foundation under Grant CCF-1336123, Grant CCF-1341966, Grant ECCS-1056065, and Grant CCF-0915994. The review of this paper was coordinated by Dr. C. Cozzo.

N. Maleki is with the Department of Electrical and Computer Engineering, University of Rochester, Rochester, NY 14627 USA (e-mail: nmalekit@ur.rochester.edu).

A. Vosoughi and N. Rahnavard are with the Department of Electrical Engineering and Computer Science, University of Central Florida, Orlando, FL 32816 USA (e-mail: azadeh@ucf.edu; nazanin@eecs.ucf.edu).

Color versions of one or more of the figures in this paper are available online at http://ieeexplore.ieee.org.

Digital Object Identifier 10.1109/TVT.2015.2497266

to the FC. In scheme 3), different from schemes 1) and 2), there is no explicit information exchange between $\mathcal{S}_1$ and $\mathcal{S}_2$. Each node forms two decisions, where one decision is made based on its observation only, and the other decision is obtained based on optimally fusing its observation with its guess of the decision of its cooperative partner. $\mathcal{S}_1$ and $\mathcal{S}_2$ apply Alamouti's scheme for transmitting these decisions to the FC. For these three schemes, we provide the likelihood ratio test (LRT) and majority fusion rules at the FC. The average (over fading) error probability of the decision error at the FC for these schemes depends on the signal-to-noise ratio (SNR) of communication (channels between cooperative partners as well as between the nodes and the FC) and sensing channels (channels between the target and the nodes). For the proposed schemes, we derive upper bounds on the average error probability and investigate how a node should allocate its transmit power for communicating with its cooperative partner and the FC, such that the error is minimized. These results enable us to quantity the cooperative gain offered by the proposed schemes, with respect to the schemes in [1] and [2], assuming identical transmit power per node.

Information exchange among the nodes for *consensus-based* distributed detection without the FC has been previously studied (examples are [14]–[17]). In [14]–[16], a consensus-based distributed detection system is considered, where the sensors successively update and broadcast their local binary decisions over *error free* links [14]–[16]. In [17], each sensor successively updates its continuous-valued decision variable and passes it to its neighbors over random links without a bandwidth constraint. Distributed detection in networks *with feedback* has been previously studied (examples are [23]–[25]) from the information-theoretic perspective, focusing on the asymptotic regime (i.e., networks with a large number of sensors) and quantifying performance in terms of error exponents. These works consider a variety of feedback architectures, including two-message feedback architectures, where each sensor sends its first message to the FC, based on its own observation, and sends its second message, based on the additional information provided by the FC through feedback, where the feedback contains (functions of) the messages generated by (some) other sensors. Different from these works, we consider networks with a finite number of sensors, without feedback from the FC, where (at most) 1-bit information exchange is allowed between two cooperative sensors. Moreover, we relax the error-free communication constraint, by considering fading effects during the information exchange phase, i.e., we assume that a sensor knows the decision of its partner with limited reliability, that is dictated by the quality of the intersensor communication channel. Perhaps the most related work is that in [22], in which each sensor communicates its local binary decision to its neighbors, and the sensors communicate their updated binary decisions to the FC. The local decision rules and the fusion rule at the FC are *all majority rules*, and communication channels are assumed to be *error free* in [22]. To the best of our knowledge, for parallel fusion architecture, no prior work has studied the impact of local (limited) information exchange on enhancing the performance of the integrated distributed detection systems [1]–[12] operating in a noisy fading environment. This paper is organized as follows. Section II introduces our sensing model and overviews the integrated distributed detection schemes in [1] and [2] for this work to be self-explanatory. Sections III–V describe schemes 1)–3), respectively, and provide local decision and fusion rules at the sensors and the FC. Section VI provides the performance analysis. Our numerical results are presented in Section VII. Concluding remarks are in Section VIII.

II. Basic Models

A. Sensing Model

We consider the binary hypothesis testing problem of detecting a known signal in correlated Gaussian noise based on measurements x_k at K distributed sensors. The *a priori* probabilities of two hypotheses $\mathcal{H}_0, \mathcal{H}_1$ are denoted by π_0, π_1, respectively. The FC is tasked with determining whether the unknown hypothesis is $\mathcal{H}_0$ or $\mathcal{H}_1$, based on the information collected from the K sensors. The measurement x_k of sensor $\mathcal{S}_k$ under $\mathcal{H}_0$ and $\mathcal{H}_1$, respectively, are $x_k = w_k$ and $x_k = 1 + w_k$ for $k = 1, \ldots, K$, where sensing noise w_k is zero mean with variance $\sigma^2_{w_k}$. The spatial correlation between noise terms w_i, w_j is characterized with the correlation coefficient ρ_{ij}. We assume that the sensors are grouped into $S = K/2$ distinct pairs of cooperative partners $(\mathcal{S}_i, \mathcal{S}_j)$, where $\mathcal{S}_i$ knows $\sigma^2_{w_i}$, $\sigma^2_{w_j}$, and ρ_{ij} only and is restricted to use the LRT. The FC employs the LRT, when all sensing noise variances and pairwise correlation coefficients are available at the FC. In the absence of this knowledge, the FC uses the majority rule.

B. Classical Parallel Fusion Architecture

Each sensor $\mathcal{S}_k$ makes a local binary decision $u_k \in \{1, -1\}$ based on its measurement x_k. The local decisions $+1$ and -1 correspond to the hypotheses $\mathcal{H}_1$ and $\mathcal{H}_0$, respectively. The local detection performance of $\mathcal{S}_k$ is characterized with $P_{d_k} = P(u_k = 1|\mathcal{H}_1)$ and $P_{f_k} = P(u_k = 1|\mathcal{H}_0)$. To form u_k, sensor $\mathcal{S}_k$ applies the LRT $(f(x_k|\mathcal{H}_1)/f(x_k|\mathcal{H}_0)) \gtrless_{u_k=-1}^{u_k=1} (\pi_0/\pi_1)$. For the sensing model in Section II-A, the LRT is reduced to $x_k \gtrless_{u_k=-1}^{u_k=1} \tau_k$, where $\tau_k = 0.5 + \sigma^2_{w_k} \ln(\pi_0/\pi_1)$. Moreover, $P_{d_k} = Q((\tau_k - 1)/\sigma_{w_k})$, and $P_{f_k} = Q(\tau_k/\sigma_{w_k})$, where $Q(x)$ denotes the Q-function.[1] The local decisions u_k are transmitted over orthogonal channels subject to noise and fading to the FC. When $\mathcal{S}_k$ sends u_k, the received signal at the FC is $y_k = u_k h_k + v_k$, where $h_k \sim \mathcal{CN}(0, \sigma^2_{h_k}), v_k \sim \mathcal{CN}(0, \sigma^2_v)$, with h_k representing the fading channel coefficient corresponding to the channel between $\mathcal{S}_k$ and the FC. The channel variance is $\sigma^2_{h_k} = \mathcal{P}\mathcal{G}/d_k^{\varepsilon}$, where $\mathcal{P}$ represents the transmit power of $\mathcal{S}_k, d_k$ denotes the distance between $\mathcal{S}_k$ and the FC, ε is the path-loss exponent, and $\mathcal{G}$ is a constant that depends on the antenna gains and the wavelength. We assume that ε and $\mathcal{G}$ are identical for all links. The term v_k is the receiver noise at the FC. We assume that v_k and h_k are independent.

[1]Considering the local LRT at sensor k, the distributions $f(x_k|\mathcal{H}_\ell)$ for $\ell = 0$, 1 and P_{d_k}, P_{f_k} values depend on the distribution of sensing noise. Thus, the simplified form of the local rule and P_{d_k}, P_{f_k} expressions would change for non-Gaussian w_k. Given the joint probability density function (pdf) $f(w_1, \ldots, w_K)$ at the FC, the expressions Λ in (1) for dependent and (2) for independent w_k's remain unchanged.

We define $\bar{\gamma}_{h_k}^2 = \sigma_{h_k}^2/\sigma_v^2$ as the average received SNR corresponding to node $\mathcal{S}_k$–FC communication channel. Relying on the received signals y_k and the availability of CSI h_k, the FC forms the LRT $\Lambda = f(y_1, \ldots, y_K|\mathcal{H}_1)/f(y_1, \ldots, y_K|\mathcal{H}_0)$, where $f(y_1, \ldots, y_K|\mathcal{H}_\ell)$ indicates the joint pdf of $y_1, \ldots, y_K$ given the hypothesis $\mathcal{H}_\ell$, to make the final decision. In particular, the FC decides on $\mathcal{H}_1$ when $\Lambda > \pi_0/\pi_1$ and decides on $\mathcal{H}_0$ otherwise. Considering that $\mathcal{H}_\ell \to u_1, \ldots, u_K \to y_1, \ldots, y_K$ form a Markov chain and the fact $f(y_1, \ldots, y_K|u_1, \ldots, u_K) = \prod_{k=1}^K f(y_k|u_k)$, we can simplify Λ as follows:

$$\Lambda = \frac{\sum_{u_1} \cdots \sum_{u_K} \left(\prod_{k=1}^K f(y_k|u_k)\right) P(u_1, \ldots, u_K|\mathcal{H}_1)}{\sum_{u_1} \cdots \sum_{u_K} \left(\prod_{k=1}^K f(y_k|u_k)\right) P(u_1, \ldots, u_K|\mathcal{H}_0)}. \tag{1}$$

Focusing on the terms $f(y_k|u_k)$ in (1), we note that given h_k, u_k, we have $y_k \sim \mathcal{CN}(u_k h_k, \sigma_v^2)$. Considering the term $P(u_1, \ldots, u_K|\mathcal{H}_\ell)$ in (1), we note that it depends on the characteristics of the sensing channel noise described in Section II-A. When Gaussian sensing noise terms are uncorrelated $\rho_{ij} = 0$ for all $i \neq j$, this term is simplified to $\prod_{k=1}^K P(u_k|\mathcal{H}_\ell)$, and (1) is reduced to [1], [2]

$$\Lambda = \prod_{k=1}^K \frac{P_{d_k} f(y_k|u_k = 1) + (1 - P_{d_k}) f(y_k|u_k = -1)}{P_{f_k} f(y_k|u_k = 1) + (1 - P_{f_k}) f(y_k|u_k = -1)}. \tag{2}$$

When the parameters of sensing channels are unavailable at the FC, the FC cannot apply the optimal LRT in (1) or (2). Alternatively, the FC demodulates the channel inputs u_k using y_k for $k = 1, \ldots, K$ and applies the majority rule to the demodulated symbols to reach the final decision, i.e., if the sum of the demodulated symbols is positive, the FC decides on $\mathcal{H}_1$ and, otherwise, decides on $\mathcal{H}_0$.

III. Cooperative Fusion Architecture With Space–Time Coding at Sensors

A. Internode Communication Channel Model and Local Decision Rules at Sensors

Suppose nodes $\mathcal{S}_i$ and $\mathcal{S}_j$ are within a pair, that is, $\mathcal{S}_i$ and $\mathcal{S}_j$ are cooperative partners. Each sensor makes a decision based on its measurement. The nodes exchange their decisions over orthogonal channels subject to noise and fading. Let u_i denote the decision made at $\mathcal{S}_i$ based on x_i. Sensor $\mathcal{S}_i$ transmits $\sqrt{1-\alpha} u_i$, where $0 < \alpha < 1$ is a power normalization factor, to assure that the total transmit power of nodes in this architecture remains the same as that of the classical parallel fusion architecture in Section II-B. When $\mathcal{S}_i$ transmits $\sqrt{1-\alpha} u_i$, the received signal at $\mathcal{S}_j$ is

$$r_{ij} = \sqrt{1-\alpha} u_i g_{ij} + \eta_{ij}$$
$$\text{where} \quad g_{ij} \sim \mathcal{CN}\left(0, \sigma_{hs_{ij}}^2\right), \quad \eta_{ij} \sim \mathcal{CN}\left(0, \sigma_\eta^2\right). \tag{3}$$

g_{ij} represents the fading channel coefficient from $\mathcal{S}_i$ to $\mathcal{S}_j$, and η_{ij} is the receiver noise at $\mathcal{S}_j$. The channel variance is $\sigma_{hs_{ij}}^2 = \mathcal{PG}/d_{ij}^\varepsilon$, where d_{ij} denotes the distance between $\mathcal{S}_i$ and $\mathcal{S}_j$. Noise terms η_{ij}, η_{ji} and channel coefficients g_{ij}, g_{ji} are independent, and noise terms are independent and identically distributed (i.i.d.) across all pairs. Upon receiving $r_{ij}, \mathcal{S}_j$ demodulates the channel input u_i, using the knowledge of g_{ij}, i.e.,

$$\hat{u}_i = \text{sgn}\left(\mathfrak{Re}\left(\frac{r_{ij}}{g_{ij}}\right)\right). \tag{4}$$

The pair $(\mathcal{S}_i, \mathcal{S}_j)$ sends the information $u_i, \hat{u}_i, u_j, \hat{u}_j$ to the FC in two consecutive time slots, exploiting Alamouti's STC scheme. In particular, in the nth slot, $\mathcal{S}_i$ and $\mathcal{S}_j$ simultaneously send $\sqrt{(\alpha/2)} u_i$ and $\sqrt{(\alpha/2)} u_j$, respectively. In the $(n+1)$th time slot, $\mathcal{S}_i$ and $\mathcal{S}_j$ simultaneously send $-\sqrt{(\alpha/2)} \hat{u}_j$ and $\sqrt{(\alpha/2)} \hat{u}_i$, respectively. Considering the definitions of channel variances, we note that, effectively, $\mathcal{S}_i$ spends $(1-\alpha)\mathcal{P}$ and $\alpha\mathcal{P} = (\alpha/2)\mathcal{P} + (\alpha/2)\mathcal{P}$, respectively, for internode and sensor–FC communication.

B. Node–FC Communication Channel Model and Fusion Rule at the FC

Let $y_{ij}(n)$ and $y_{ij}(n+1)$ denote the received signals at the FC corresponding to the pair $(\mathcal{S}_i, \mathcal{S}_j)$ during two consecutive time slots. We have

$$y_{ij}(n) = \sqrt{\frac{\alpha}{2}}(u_i h_i + u_j h_j) + v_{ij}(n)$$
$$y_{ij}(n+1) = \sqrt{\frac{\alpha}{2}}(-\hat{u}_j h_i + \hat{u}_i h_j) + v_{ij}(n+1) \tag{5}$$

where $h_{i(j)} \sim \mathcal{CN}(0, \sigma_{h_{i(j)}}^2), v_{ij}(n), v_{ij}(n+1) \sim \mathcal{CN}(0, \sigma_v^2)$. The term $v_{ij}(n)$ is the receiver noise at the FC during the nth time slot. We assume that noise terms $v_{ij}(n), v_{ij}(n+1)$ and channel coefficients h_i, h_j are independent, and noise terms are i.i.d. across all pairs. Taking similar processing as Alamouti decoding [20], the FC first forms z_i, z_j using $y_{ij}(n), y_{ij}^*(n+1)$ as follows:

$$\begin{aligned}
\begin{bmatrix} z_i \\ z_j \end{bmatrix} &= \begin{bmatrix} h_i^* & h_j \\ h_j^* & -h_i \end{bmatrix} \begin{bmatrix} y_{ij}(n) \\ y_{ij}^*(n+1) \end{bmatrix} \\
&= \begin{bmatrix} h_i^* & h_j \\ h_j^* & -h_i \end{bmatrix} \begin{bmatrix} v_{ij}(n) \\ v_{ij}^*(n+1) \end{bmatrix} \\
&\quad + \sqrt{\frac{\alpha}{2}} \left(\begin{bmatrix} |h_i|^2 & h_j h_i^* \\ h_i h_j^* & |h_j|^2 \end{bmatrix} \begin{bmatrix} u_i \\ u_j \end{bmatrix} \right. \\
&\quad \left. + \begin{bmatrix} |h_j|^2 & -h_j h_i^* \\ -h_i h_j^* & |h_i|^2 \end{bmatrix} \begin{bmatrix} \hat{u}_i \\ \hat{u}_j \end{bmatrix} \right).
\end{aligned}$$

Note that if each node allocates equal power for communicating with its cooperative partner and with the FC, i.e., $\alpha = 1/2$, and there is no error during internode communication, i.e., $\hat{u}_i = u_i$, $\hat{u}_j = u_j$, the given equations reduce to the classical Alamouti's scheme [20]. The new noise terms $\delta_{ij}^1 = h_i^* v_{ij}(n) + h_j v_{ij}^*(n+1)$ and $\delta_{ij}^2 = h_j^* v_{ij}(n) - h_i v_{ij}^*(n+1)$ are i.i.d. zero-mean complex Gaussian random variables (RVs) with the variance $\sigma^2 = (|h_i|^2 + |h_j|^2)\sigma_v^2$. Next, using the signals z_i, z_j and the CSI h_i, h_j for all pairs, the FC forms the LRT $\Lambda = (f(z_i, z_j \text{ for all pairs}|\mathcal{H}_1)/f(z_i, z_j \text{ for all pairs}|\mathcal{H}_0))$, where $f(z_i, z_j \text{ for all pairs}|\mathcal{H}_\ell)$ indicates the joint pdf of z_i, z_j corresponding to all pairs given the hypothesis $\mathcal{H}_\ell$, to make the final decision. In particular, the FC decides on $\mathcal{H}_1$ when $\Lambda > \pi_0/\pi_1$ and decides on $\mathcal{H}_0$ otherwise. We note that $\mathcal{H}_\ell \rightarrow u_i, u_j, \hat{u}_i, \hat{u}_j \rightarrow z_i, z_j$ and $\mathcal{H}_\ell \rightarrow u_i, u_j \rightarrow \hat{u}_i, \hat{u}_j$ form Markov chains. Moreover, (z_i, z_j) values are independent across the pairs given $u_i, u_j, \hat{u}_i, \hat{u}_j$ for all pairs. Furthermore, given u_i, u_j for for all pairs, $(\hat{u}_i, \hat{u}_j)$ values are independent across the pairs. Therefore, we write

$$
\begin{aligned}
&f(z_i, z_j \text{ for all pairs}|\mathcal{H}_\ell) = \sum_{u_i}\sum_{u_j}\sum_{\hat{u}_i}\sum_{\hat{u}_j} \\
&f(z_i, z_j \text{ for all pairs}|u_i, u_j, \hat{u}_i, \hat{u}_j \text{ for all pairs}) \\
&\qquad \times P(u_i, u_j, \hat{u}_i, \hat{u}_j \text{ for all pairs}|\mathcal{H}_\ell) \\
&= \sum_{u_i}\sum_{\hat{u}_i}\sum_{u_j}\sum_{\hat{u}_j}\Bigg(\prod_{\text{for all pairs}} f(z_i, z_j|u_i, u_j, \hat{u}_i, \hat{u}_j \text{ for } (\mathcal{S}_i, \mathcal{S}_j)) \\
&\qquad \times P(\hat{u}_i|u_i \text{ for } (\mathcal{S}_i, \mathcal{S}_j)) P(\hat{u}_j|u_j \text{ for } (\mathcal{S}_i, \mathcal{S}_j))\Bigg) \\
&\qquad \times P(u_i, u_j \text{ for all pairs}|\mathcal{H}_\ell) \qquad (6)
\end{aligned}
$$

where the sums are taken over all values that $u_i, u_j, \hat{u}_i, \hat{u}_j$ can assume. Focusing on $f(z_i, z_j|u_i, u_j, \hat{u}_i, \hat{u}_j \text{ for } (\mathcal{S}_i, \mathcal{S}_j))$ in (6), we realize that z_i, z_j values are conditionally independent complex Gaussian RVs with the variance $\sigma^2 = (|h_i|^2 + |h_j|^2)\sigma_v^2$, and the mean values μ_i, μ_j are given in the following equation:

$$
\begin{aligned}
\mu_i &= \sqrt{\frac{\alpha}{2}}\left(|h_i|^2 u_i + h_j h_i^* u_j + |h_j|^2 \hat{u}_i - h_j h_i^* \hat{u}_j\right) \\
\mu_j &= \sqrt{\frac{\alpha}{2}}\left(h_i h_j^* u_i + |h_j|^2 u_j - h_i h_j^* \hat{u}_i + |h_i|^2 \hat{u}_j\right). \qquad (7)
\end{aligned}
$$

Focusing on the term $P(\hat{u}_i|u_i \text{ for } (\mathcal{S}_i, \mathcal{S}_j))$ in (6) and considering (4), one can easily verify the following, assuming that the FC only knows the statistics of internode channels g_{ij}, g_{ji} [23]. Thus

$$
P(\hat{u}_i \neq u_i|u_i) = 1 - P(\hat{u}_i = u_i|u_i) = \frac{1}{2}\left(1 - \sqrt{\frac{\bar{\gamma}_{hs_{ij}}}{1 + \bar{\gamma}_{hs_{ij}}}}\right)
$$
$$
\text{where} \qquad \bar{\gamma}_{hs_{ij}} = \frac{(1-\alpha)\sigma^2_{hs_{ij}}}{\sigma^2_\eta} \qquad (8)
$$

denotes the average received SNR corresponding to $(\mathcal{S}_i, \mathcal{S}_j)$ internode communication. The term $P(u_i, u_j \text{ for all pairs}|\mathcal{H}_\ell)$ in (6) can be found in terms of the probability of x_i, x_j being in certain intervals for all pairs. For instance, $P(u_i = 1, u_j = -1 \text{ for all pairs}|\mathcal{H}_\ell) = P(x_i > \tau_i, x_j < \tau_j \text{ for all pairs}|\mathcal{H}_\ell)$. These probabilities can be characterized for the sensing channel model in Section II-A, where x_i, x_j values are jointly correlated Gaussian RVs with known statistics.[2] When Gaussian sensing noise terms are uncorrelated, we obtain $P(u_i = 1, u_j = -1 \text{ for all pairs}|\mathcal{H}_0) = \prod_{\{i:u_i=1\}} P_{f_i} \prod_{\{j:u_j=-1\}}(1 - P_{f_j})$ or $P(u_i = 1, u_j = -1 \text{ for all pairs}|\mathcal{H}_1) = \prod_{\{i:u_i=1\}} P_{d_i} \prod_{\{j:u_j=-1\}}(1 - P_{d_j})$. When the parameters of sensing channels are unavailable at the FC, the FC cannot apply the LRT. Alternatively, the FC demodulates the channel inputs for all pairs using the signals z_i, z_j for all pairs and applies the majority rule to the demodulated symbols to reach the final decision.

[2]For non-Gaussian w_k's, the probability $P(u_i, u_j \text{ for all pairs}|\mathcal{H}_\ell)$ should be calculated in terms of the joint pdf $f(w_1, \ldots, w_K)$.

IV. Cooperative Fusion Architecture With Signal Fusion at Sensors

A. *Internode Communication Channel Model and Local Decision Rules at Sensors*

Suppose nodes $\mathcal{S}_i$ and $\mathcal{S}_j$ are within a pair. Each sensor makes an initial decision based on its measurement. The nodes exchange their decisions over orthogonal channels subject to noise and fading. Let u_i denote the decision made at $\mathcal{S}_i$ based on x_i. When $\mathcal{S}_i$ transmits $\sqrt{1-\alpha}u_i$, the received signal at $\mathcal{S}_j$ is r_{ij}, as shown in (3). Upon receiving $r_{ij}, \mathcal{S}_j$ (rather than demodulating the channel input) updates its initial decision by fusing r_{ij} and its measurement x_j. In particular, $\mathcal{S}_j$ forms a local LRT $\tilde{\lambda}_j = f(r_{ij}, x_j|\mathcal{H}_1)/f(r_{ij}, x_j|\mathcal{H}_0)$, where $f(r_{ij}, x_j|\mathcal{H}_\ell)$ indicates the joint pdf of r_{ij}, x_j given the hypothesis $\mathcal{H}_\ell$, to make a new decision $\tilde{u}_j$. Node $\mathcal{S}_j$ lets $\tilde{u}_j = 1$ when $\tilde{\lambda}_j > \pi_0/\pi_1$ and lets $\tilde{u}_j = -1$ otherwise. Since $\mathcal{H}_\ell \rightarrow u_i \rightarrow r_{ij}$ and $x_j \rightarrow \mathcal{H}_\ell, u_i \rightarrow r_{ij}$ form Markov chains, we find

$$
\tilde{\lambda}_j = \frac{\sum_{u_i} f(r_{ij}|u_i)P(u_i|x_j, \mathcal{H}_1)f(x_j|\mathcal{H}_1)}{\sum_{u_i} f(r_{ij}|u_i)P(u_i|x_j, \mathcal{H}_0)f(x_j|\mathcal{H}_0)}. \qquad (9)
$$

Considering $f(r_{ij}|u_i)$ in (9), we note that given g_{ij}, u_i, we have $r_{ij} \sim \mathcal{CN}(\sqrt{1-\alpha}u_i g_{ij}, \sigma^2_\eta)$. To find $P(u_i|x_j, \mathcal{H}_\ell)$ in (9), we note that for the sensing model in Section II-A, x_i, x_j values are jointly Gaussian RVs with mean ℓ, variances $\sigma^2_{w_i}, \sigma^2_{w_j}$, and correlation coefficient $\rho_{i,j}$ under the hypothesis $\mathcal{H}_\ell$. Using the joint pdf of x_i, x_j and the Bayes' rule $P(u_i = 1|x_j, \mathcal{H}_\ell) = (P(u_i = 1, x_j|\mathcal{H}_\ell)/f(x_j|\mathcal{H}_\ell))$, one can show

$$
\begin{aligned}
P(u_i = 1|x_j, \mathcal{H}_\ell) &= 1 - P(u_i = -1|x_j, \mathcal{H}_\ell) \\
&= Q\left(\frac{\tau_i - \rho_{i,j} x_j \frac{\sigma_{w_i}}{\sigma_{w_j}} - \ell\left(1 - \rho_{i,j}\frac{\sigma_{w_i}}{\sigma_{w_j}}\right)}{\sqrt{\left(1 - \rho^2_{i,j}\right)}\sigma_{w_i}}\right). \qquad (10)
\end{aligned}
$$

Finally, we find $f(x_j|\mathcal{H}_\ell)$ in (9) by noting that given $\mathcal{H}_\ell$, we have $x_j \sim \mathcal{CN}(\ell, \sigma^2_{w_j})$. When Gaussian sensing noise terms are uncorrelated, u_i and x_j are independent[3] for a given hypothesis $\mathcal{H}_\ell$, leading to $P(u_i|x_j, \mathcal{H}_\ell) = P(u_i|\mathcal{H}_\ell)$. The pair $(\mathcal{S}_i, \mathcal{S}_j)$ sends $\sqrt{\alpha}\tilde{u}_i, \sqrt{\alpha}\tilde{u}_j$ to the FC over two orthogonal channels subject to noise and fading. Considering the definitions of channel variances, we note that, effectively, $\mathcal{S}_i$ spends $(1-\alpha)\mathcal{P}$ and $\alpha\mathcal{P}$, respectively, for internode and sensor–FC communication.

[3]For non-Gaussian sensing noise terms, when forming $\tilde{\lambda}_j$, $P(u_i|x_j, \mathcal{H}_\ell)$ and $f(x_j|\mathcal{H}_\ell)$ should be calculated, respectively, based on the joint pdf $f(w_i, w_j)$ and the pdf $f(w_j)$. Moreover, $P(u_i|x_j, \mathcal{H}_\ell) = P(u_i|\mathcal{H}_\ell)$ when w_i, w_j values are mutually independent.

B. Node–FC Communication Channel Model and Fusion Rule at the FC

Let y_i and y_j denote the received signals at the FC corresponding to the pair $(\mathcal{S}_i, \mathcal{S}_j)$. We have

$$y_i = \sqrt{\alpha}\tilde{u}_i h_i + v_i, \quad y_j = \sqrt{\alpha}\tilde{u}_j h_j + v_j$$
$$h_{i(j)} \sim \mathcal{CN}\left(0, \sigma^2_{h_{i(j)}}\right), v_i, \quad v_j \sim \mathcal{CN}\left(0, \sigma_v^2\right).$$

The terms v_i and v_j are the receiver noise at the FC. We assume that noise and fading coefficients are independent, and noise terms are i.i.d. across the pairs. Next, using the signals y_i, y_j and the CSI h_i, h_j for all pairs, the FC forms the LRT $\Lambda = (f(y_i, y_j \text{ for all pairs}|\mathcal{H}_1)/f(y_i, y_j \text{ for all pairs}|\mathcal{H}_0))$, where $f(y_i, y_j \text{ for all pairs}|\mathcal{H}_\ell)$ indicates the joint pdf of y_i, y_j corresponding to all pairs given the hypothesis $\mathcal{H}_\ell$, to make the final decision. We note that $\mathcal{H}_\ell \to \tilde{u}_i, \tilde{u}_j \to y_i, y_j$ form a Markov chain. Furthermore, (y_i, y_j) values are independent across the pairs given $\tilde{u}_i, \tilde{u}_j$ for all pairs. Hence, we can write

$$\begin{aligned} f(y_i, y_j \text{ for all pairs}|\mathcal{H}_\ell) &= \sum_{\tilde{u}_i}\sum_{\tilde{u}_j} \\ &(P(\tilde{u}_i, \tilde{u}_j \text{ for all pairs}|\mathcal{H}_\ell) \\ &\quad \times f(y_i, y_j \text{ for all pairs}|\tilde{u}_i, \tilde{u}_j \text{ for all pairs })) \\ &= \sum_{\tilde{u}_i}\sum_{\tilde{u}_j}\left(\prod_{\text{for all pairs}} f(y_i, y_j|\tilde{u}_i, \tilde{u}_j \text{ for } (\mathcal{S}_i, \mathcal{S}_j))\right) \\ &\quad \times P(\tilde{u}_i, \tilde{u}_j \text{ for all pairs}|\mathcal{H}_\ell) \end{aligned} \tag{11}$$

where the sums are taken over all values that $\tilde{u}_i, \tilde{u}_j$ can take. To find $f(y_i, y_j|\tilde{u}_i, \tilde{u}_j \text{ for } (\mathcal{S}_i, \mathcal{S}_j))$ in (11), we realize that in the pair $(\mathcal{S}_i, \mathcal{S}_j)$ given $\tilde{u}_i, \tilde{u}_j$, the variables y_i and y_j are independent complex Gaussian RVs with mean values $\mu_i = \sqrt{\alpha}\tilde{u}_i h_i$ and $\mu_j = \sqrt{\alpha}\tilde{u}_j h_j$ and variance σ_v^2. To obtain $P(\tilde{u}_i, \tilde{u}_j \text{ for all pairs}|\mathcal{H}_\ell)$ in (11), we assume that the FC only knows the statistics of internode channels g_{ij}, g_{ji}. Note that $\mathcal{H}_\ell \to x_i, x_j, r_{ij}, r_{ji} \to \tilde{u}_i, \tilde{u}_j$ forms a Markov chain. Therefore

$$\begin{aligned} P(\tilde{u}_i, \tilde{u}_j \text{ for all pairs}|\mathcal{H}_\ell) &= \int_{g_{ij}}\int_{g_{ji}}\int_{x_i}\int_{x_j}\int_{r_{ij}}\int_{r_{ji}} \\ &P(\tilde{u}_i, \tilde{u}_j \text{ for all pairs}|g_{ij}, g_{ji}, x_i, x_j, r_{ij}, r_{ji} \text{ for all pairs}) \\ &\quad \times f(x_i, x_j, r_{ij}, r_{ji} \text{ for all pairs}|\mathcal{H}_\ell) \\ &\quad \times f(g_{ij}, g_{ji}) dg_{ij} dg_{ji} dx_i dx_j dr_{ij} dr_{ji}. \end{aligned} \tag{12}$$

Equation (12) can be further simplified by noting that given x_i, x_j, r_{ij}, r_{ji} for all pairs, the variables $(\tilde{u}_i, \tilde{u}_j)$ are independent across the pairs. Furthermore, within a pair, given x_i, x_j, r_{ij}, r_{ji}, variables $\tilde{u}_i$ and $\tilde{u}_j$ are independent. In addition, we note that $\mathcal{H}_\ell \to x_i, x_j \to r_{ij}, r_{ji}$ forms a Markov chain, and given x_i, x_j for all pairs, (r_{ij}, r_{ji}) values are independent across the pairs. Moreover, within a pair, given x_i, x_j, variables r_{ij}, r_{ji} are independent. Combining all, we can rewrite (12) as (13), shown at the bottom of the page.

Focusing on the term $P(\tilde{u}_i|x_i, r_{ji} \text{ for } (\mathcal{S}_i, \mathcal{S}_j))$ in (13), we note that $P(\tilde{u}_i = 1|x_i, r_{ji}) = \mathbf{1}_{\{\tilde{\lambda}_i > \pi_0/\pi_1\}}$ and $P(\tilde{u}_i = -1|x_i, r_{ji}) = \mathbf{1}_{\{\tilde{\lambda}_i < \pi_0/\pi_1\}}$, where $\tilde{\lambda}_i$ depends on internode channels g_{ji}, threshold τ_j, sensing noise variances $\sigma^2_{w_i}, \sigma^2_{w_j}$, and correlation coefficient $\rho_{i,j}$. Similarly, we can find $P(\tilde{u}_j|x_j, r_{ij} \text{ for } (\mathcal{S}_i, \mathcal{S}_j))$ in (13). Considering the term $f(r_{ji}|x_j \text{ for } (\mathcal{S}_i, \mathcal{S}_j))$ in (13), we find

$$\begin{aligned} &f(r_{ji}|x_j \text{ for } (\mathcal{S}_i, \mathcal{S}_j)) \\ &\quad = f(r_{ji}|u_j = 1)P(u_j = 1|x_j) + f(r_{ji}|u_j = -1)P(u_j = -1|x_j) \\ &\quad = f(r_{ji}|u_j = 1)\mathbf{1}_{\{x_j > \tau_j\}} + f(r_{ji}|u_j = -1)\mathbf{1}_{\{x_j < \tau_j\}} \end{aligned} \tag{14}$$

where $f(r_{ji}|u_j)$ in (14) can be found noting that given g_{ji}, u_j, we have $r_{ji} \sim \mathcal{CN}(\sqrt{1-\alpha}u_j g_{ji}, \sigma_\eta^2)$. Considering the term $f(x_i, x_j \text{ for all pairs}|\mathcal{H}_\ell)$ in (13), we note that when Gaussian sensing noise terms are uncorrelated[4] we obtain $f(x_i, x_j \text{ for all pairs}|\mathcal{H}_\ell) = \prod_{\text{for all pairs}} f(x_i \text{ for } (\mathcal{S}_i, \mathcal{S}_j)|\mathcal{H}_\ell)$ $f(x_j \text{ for } (\mathcal{S}_i, \mathcal{S}_j)|\mathcal{H}_\ell)$. Combining all these, one can verify that the probability in (12) depends on sensing channels through $\tau_i, \tau_j, \sigma^2_{w_i}, \sigma^2_{w_j}, \rho_{i,j}$ and the average received SNR $\bar{\gamma}_{hs_{ij}}$ corresponding to $(\mathcal{S}_i, \mathcal{S}_j)$ internode communication. When the parameters of sensing channels are unavailable at the FC, the FC demodulates the channel inputs for all pairs using the signals y_i, y_j for all pairs and applies the majority rule to the demodulated symbols to reach the final decision.

V. Parallel Fusion Architecture With Local Threshold Changing at Sensors

A. Local Decision Rules at Sensors

Suppose nodes $\mathcal{S}_i$ and $\mathcal{S}_j$ are within a pair. Each sensor makes an initial decision based on its measurement. Let u_i denote the decision made at $\mathcal{S}_i$ based on x_i. In the absence of internode communication, $\mathcal{S}_i$ assumes that the decision u_j (made at $\mathcal{S}_j$ based on x_j) is different from u_i, i.e., $\mathcal{S}_i$ assumes $u_j = -u_i$. Next, $\mathcal{S}_i$ forms another decision $\bar{u}_i$ by fusing the

[4]For non-Gaussian sensing noise, $\tilde{\lambda}_i$ would change, as explained in the previous footnote. Moreover, $P(u_j|x_j)$ in (14) and $f(x_i, x_j \text{ for all pairs}|\mathcal{H}_\ell)$ in (13), respectively, should be calculated based on the pdf $f(w_j)$ and the joint pdf $f(w_1, \ldots, w_K)$.

$$\begin{aligned} &\int_{g_{ij}}\int_{g_{ji}}\int_{x_i}\int_{x_j}\int_{r_{ij}}\int_{r_{ji}}\left(\prod_{\text{for all pairs}} P(\tilde{u}_i|x_i, r_{ji} \text{ for } (\mathcal{S}_i, \mathcal{S}_j))\, P(\tilde{u}_j|x_j, r_{ij} \text{ for } (\mathcal{S}_i, \mathcal{S}_j)) \times f(r_{ji}|x_j \text{ for } (\mathcal{S}_i, \mathcal{S}_j))\, f(r_{ij}|x_i \text{ for } (\mathcal{S}_i, \mathcal{S}_j))\right) \\ &\qquad \times f(x_i, x_j \text{ for all pairs }|\mathcal{H}_\ell) f(g_{ij}, g_{ji}) dg_{ij} dg_{ji} dx_i dx_j dr_{ij} dr_{ji} \end{aligned} \tag{13}$$

assumed decision u_j and its measurement x_i. In particular, $\mathcal{S}_i$ forms a local LRT $\bar{\lambda}_i = f(x_i, u_j = -u_i|\mathcal{H}_1)/f(x_i, u_j = -u_i|\mathcal{H}_0)$, where $f(x_i, u_j = -u_i|\mathcal{H}_\ell)$ indicates the joint pdf of x_i and the assumed decision u_j at $\mathcal{S}_i$ given the hypothesis $\mathcal{H}_\ell$, to make $\bar{u}_i$. Node $\mathcal{S}_i$ lets $\bar{u}_i = 1$ when $\bar{\lambda}_i > \pi_0/\pi_1$ and lets $\bar{u}_i = -1$ otherwise. We find[5]

$$\bar{\lambda}_i = \frac{P(u_j = -u_i|x_i, \mathcal{H}_1) f(x_i|\mathcal{H}_1)}{P(u_j = -u_i|x_i, \mathcal{H}_0) f(x_i|\mathcal{H}_0)} \tag{15}$$

in which $P(u_j = -u_i|x_i, \mathcal{H}_\ell)$ is given in (10), and $f(x_j|\mathcal{H}_\ell)$ is found by noting[6] that given $\mathcal{H}_\ell$, we have $x_j \sim \mathcal{CN}(\ell, \sigma^2_{w_j})$. In fact, one can verify that $\mathcal{S}_i$ finds $u_i, \bar{u}_i$, as follows:

$$\begin{cases} u_i = 1, \bar{u}_i = 1, & \text{if } x_i > \tau'_{i_1} \\ u_i = -1, \bar{u}_i = -1, & \text{if } x_i < \tau'_{i_2} \\ u_i = -1, \bar{u}_i = 1, & \text{if } \tau'_{i_2} < x_i < \tau_i \\ u_i = 1, \bar{u}_i = -1, & \text{if } \tau_i < x_i < \tau'_{i_1} \end{cases} \tag{16}$$

where the thresholds τ'_{i_1}, τ'_{i_2}, given in the footnote, depend on $\sigma^2_{w_i}, \rho_{i,j}$ and satisfy $\tau'_{i_2} < \tau_i < \tau'_{i_1}$. When Gaussian sensing noise terms are uncorrelated, the assumed decision u_j and x_i are independent for a given hypothesis $\mathcal{H}_\ell$, leading to $P(u_j = -u_i|x_i, \mathcal{H}_\ell) = P(u_j = -u_i|\mathcal{H}_\ell)$ in (15). Consequently, the local LRT $\bar{\lambda}_i$ in (15) can be further simplified, and τ'_{i_1}, τ'_{i_2} in (16), respectively, reduce to $\tau_{i_1} = 0.5 + \sigma^2_{w_i} \ln((1 - P_{f_j})\pi_0/(1 - P_{d_j})\pi_1)$ and $\tau_{i_2} = 0.5 + \sigma^2_{w_i} \ln(P_{f_j}\pi_0/P_{d_j}\pi_1)$, where $\tau_{i_2} < \tau_i < \tau_{i_1}$. Since, in addition to threshold τ_i employed in scheme 1), x_i is also compared against two additional thresholds τ'_{i_1}, τ'_{i_2}, we refer to scheme 3) as "local threshold changing." The pair $(\mathcal{S}_i, \mathcal{S}_j)$ sends $u_i, \bar{u}_i, u_j, \bar{u}_j$ to the FC in two consecutive time slots, exploiting Alamouti's STC scheme. In particular, in the nth slot, $\mathcal{S}_i$ and $\mathcal{S}_j$ can simultaneously send $(u_i/\sqrt{2})$ and $(\bar{u}_j/\sqrt{2})$, respectively. In the $(n+1)$th time slot, $\mathcal{S}_i$ and $\mathcal{S}_j$ can simultaneously send $-(\bar{u}_i/\sqrt{2})$ and $(u_j/\sqrt{2})$, respectively. Considering the definitions of channel variances, we note that, effectively, $\mathcal{S}_i$ spends $\mathcal{P} = (1/2)\mathcal{P} + (1/2)\mathcal{P}$ for sensor–FC communication.

[5]Consider a hypothetical case where $\mathcal{S}_i$ assumes $u_j = -1$ and makes a decision u^0_i by optimally fusing the assumed $u_j = -1$ and x_i. In particular, $\mathcal{S}_i$ lets $u^0_i = 1$ when $\lambda^0_i = (f(x_i, u_j = -1|\mathcal{H}_1)/f(x_i, u_j = -1|\mathcal{H}_0)) > (\pi_0/\pi_1)$ and lets $u^0_i = -1$ otherwise. Consider another hypothetical case where $\mathcal{S}_i$ assumes $u_j = 1$ and makes a decision u^1_i by optimally fusing the assumed $u_j = 1$ and x_i. In particular, $\mathcal{S}_i$ lets $u^1_i = 1$ when $\lambda^1_i = (f(x_i, u_j = 1|\mathcal{H}_1)/f(x_i, u_j = 1|\mathcal{H}_0)) > (\pi_0/\pi_1)$ and lets $u^1_i = -1$ otherwise. One can verify $u^0_i = 1$ when $x_i > \tau'_{i_1}$ and $u^0_i = -1$ otherwise, also $u^1_i = 1$ when $x_i > \tau'_{i_2}$ and $u^1_i = -1$ otherwise, where $\tau'_{i_1} = 0.5 + \sigma^2_{w_i} \ln(P(u_j = -1|x_i, \mathcal{H}_0)\pi_0/P(u_j = -1|x_i, \mathcal{H}_1)\pi_1)$ and $\tau'_{i_2} = 0.5 + \sigma^2_{w_i} \ln(P(u_j = 1|x_i, \mathcal{H}_0)\pi_0/P(u_j = 1|x_i, \mathcal{H}_1)\pi_1)$ and $\tau'_{i_2} < \tau_i < \tau'_{i_1}$. For these hypothetical cases, now suppose $x_i < \tau_i$, and thus, $u_i = -1$. Since $\tau_i < \tau'_{i_1}$, we have $x_i < \tau'_{i_1}$, and thus, $u^0_i = -1$, i.e., $u^0_i = u_i$, whereas u^1_i can ± 1. Therefore, the useful information is embedded in u_i, u^1_i, as u^0_i conveys no extra information. Similarly, one can argue that when $x_i > \tau_i$, the useful information is imbedded in u_i, u^0_i, as u^1_i does not convey extra information. In conclusion, node $\mathcal{S}_i$ should assume $u_j = -u_i$ to be able to extract more information from x_i.

[6]For non-Gaussian sensing noise, similar to $\tilde{\lambda}_i$ in Section IV-A, $\bar{\lambda}_i$ would change. In particular, $P(u_j|x_i, \mathcal{H}_\ell)$ and $f(x_i|\mathcal{H}_\ell)$ should be calculated, respectively, based on the joint pdf $f(w_i, w_j)$ and the pdf $f(w_i)$.

B. Node–FC Communication Channel Model and Fusion Rule at FC

Let $y_{ij}(n)$ and $y_{ij}(n+1)$ denote the received signals at the FC corresponding to the pair $(\mathcal{S}_i, \mathcal{S}_j)$ during two consecutive time slots. The signal model in (5) still holds true, after substituting $\sqrt{\alpha/2}$ with $1/\sqrt{2}$, u_j with $\bar{u}_j$, $\hat{u}_j$ with $\bar{u}_i$, and $\hat{u}_i$ with u_j. We can take similar steps as in Section III-B to find the signals z_i, z_j using $y_{ij}(n), y^*_{ij}(n+1)$. Next, using the signals z_i, z_j and the CSI h_i, h_j for all pairs, the FC forms the LRT $\Lambda = (f(z_i, z_j \text{ for all pairs}|\mathcal{H}_1)/f(z_i, z_j \text{ for all pairs}|\mathcal{H}_0))$. We note that $\mathcal{H}_\ell \to u_i, u_j, \bar{u}_i, \bar{u}_j \to z_i, z_j$ forms a Markov chain. Moreover, (z_i, z_j) values are independent across the pairs given $u_i, u_j, \bar{u}_i, \bar{u}_j$ for all pairs. Therefore, we reach (17), shown at the bottom of the page.

Focusing on the term $f(z_i, z_j|u_i, u_j, \bar{u}_i, \bar{u}_j \text{ for } (\mathcal{S}_i, \mathcal{S}_j))$ in (17), we realize that z_i, z_j values are conditionally independent complex Gaussian RVs with variance $\sigma^2 = (|h_i|^2 + |h_j|^2)\sigma^2_v$ and mean values μ_i, μ_j given in (7), after substituting $\sqrt{(\alpha/2)}$ with $(1/\sqrt{2})$, u_j with $\bar{u}_j$, $\hat{u}_j$ with $\bar{u}_i$, and $\hat{u}_i$ with u_j. To find $P(u_i, u_j, \bar{u}_i, \bar{u}_j \text{ for all pairs}|\mathcal{H}_\ell)$, we note that this term can be expressed in terms of the probability of x_i, x_j being in certain intervals for all pairs. For instance, $P(u_i = \bar{u}_i = 1, u_j = \bar{u}_j = -1 \text{ for all pairs}|\mathcal{H}_\ell) = P(x_i > \tau_{ij_1}, x_j < \tau_{ij_2} \text{ for all pairs}|\mathcal{H}_\ell)$. Now, these probabilities can be easily characterized for the sensing channel model in Section II-A, where x_i, x_j values are jointly correlated Gaussian RVs with known statistics.[7] When Gaussian sensing noise terms are uncorrelated, the decisions $(u_i, \bar{u}_i)$ and $(u_j, \bar{u}_j)$ given hypothesis $\mathcal{H}_\ell$ are independent across the pairs. Therefore, $P(u_i, u_j, \bar{u}_i, \bar{u}_j \text{ for all pairs}|\mathcal{H}_\ell) = \prod_{\text{for all pairs}} P(u_i, \bar{u}_i \text{ for } (\mathcal{S}_i, \mathcal{S}_j)|\mathcal{H}_\ell) \times P(u_j, \bar{u}_j \text{ for } (\mathcal{S}_i, \mathcal{S}_j)|\mathcal{H}_\ell)$. When the parameters of sensing channels are unavailable at the FC, the FC demodulates the channel inputs for all pairs using the signals z_i, z_j for all pairs and applies the majority rule to the demodulated symbols to reach the final decision.

[7]For non-Gaussian w_k's, $P(u_i, u_j, \bar{u}_i, \bar{u}_j \text{ for all pairs}|\mathcal{H}_\ell)$ should be calculated in terms of the joint pdf $f(w_1, \ldots, w_K)$.

$$f(z_i, z_j \text{ for all pairs}|\mathcal{H}_\ell) = \sum_{u_i \text{ for all pairs}} \sum_{u_j \text{ for all pairs}} \sum_{\bar{u}_i \text{ for all pairs}} \sum_{\bar{u}_j \text{ for all pairs}} \times \left(\prod_{\text{for all pairs}} f\left(z_i, z_j|u_i, u_j, \bar{u}_i, \bar{u}_j \text{ for } (\mathcal{S}_i, \mathcal{S}_j)\right) \right) \times P(u_i, u_j, \bar{u}_i, \bar{u}_j \text{ for all pairs}|\mathcal{H}_\ell) \tag{17}$$

VI. Performance Analysis

Section VI-A provides an upper bound on the average error probability for scheme 1) in Section III. Leveraging on this, Section VI-B and C, respectively, provide upper bounds on the average error probability for the classical parallel fusion architecture in Section II-B and scheme 2) in Section IV. For mathematical tractability, we assume that the Gaussian sensing noise terms w_k are identically distributed and uncorrelated,[8] i.e., we have $\sigma^2_{w_k} = \sigma^2_w$, and $\tau_k = \tau$, and thus, $P_{d_k} = P_d$, and $P_{f_k} = P_f$. Moreover, we assume that sensors are positioned equally distant from the FC, and thus, $\bar{\gamma}^2_h = (\sigma^2_h/\sigma^2_v)$. Furthermore, distances between the cooperative partners are assumed equal across the pairs, and therefore, $\bar{\gamma}^2_{hs} = ((1-\alpha)\sigma^2_{hs}/\sigma^2_\eta)$. In Section VII, we validate the analytical results of this section via Monte Carlo simulations.

A. Cooperative Fusion Architecture With STC at Sensors

For performance analysis, suppose each pair of cooperative partners $(\mathcal{S}_i, \mathcal{S}_j)$ is associated with a unique group index s, where $s = 1, \ldots, S$ and $S = K/2$. We denote the two nodes within group s as $(\mathcal{S}_{2s-1}, \mathcal{S}_{2s})$, i.e., we map the indexes i, j in Section III into $2s-1, 2s$, respectively. For the LRT fusion rule in Section III-B, the conditional error probability is $P_{e|h} = P_{e_1|h} + P_{e_2|h}$, where $P_{e_1|h} = P(\Lambda > (\pi_0/\pi_1)|\mathcal{H}_0)\pi_0$ and $P_{e_2|h} = P(\Lambda < (\pi_0/\pi_1)|\mathcal{H}_1)\pi_1$ and $\Lambda = (f(z_{2s-1}, z_{2s} \text{ for } s = 1, \ldots, S|\mathcal{H}_1)/f(z_{2s-1}, z_{2s} \text{ for } s = 1, \ldots, S|\mathcal{H}_0))$, conditioned on the channel coefficients h_{2s-1}, h_{2s} for $s = 1, \ldots, S$ at the FC. The average error probability $\bar{P}_e = \bar{P}_{e_1} + \bar{P}_{e_2}$ is obtained by taking the averages of $P_{e_1|h}, P_{e_2|h}$ over the distribution of the channel coefficients. Our goal is to provide upper bounds on $P_{e_1|h}, P_{e_2|h}$ and their corresponding averages $\bar{P}_{e_1} = \mathbb{E}\{P_{e_1|h}\}, \bar{P}_{e_2} = \mathbb{E}\{P_{e_2|h}\}$. We use the following notation in our derivations. To capture all different values that $u_{2s-1}, u_{2s}, \hat{u}_{2s-1}, \hat{u}_{2s}$ for $s = 1, \ldots, S$ can take, we consider two K-length sequences $(a^1_{n_1}, \ldots, a^{2s-1}_{n_1}, a^{2s}_{n_1}, \ldots, a^{2S}_{n_1})$ and $(a^1_{m_1}, \ldots, a^{2s-1}_{m_1}, a^{2s}_{m_1}, \ldots, a^{2S}_{m_1})$, where $a^{2s-1}_{n_1}, a^{2s}_{n_1} \in \{1, -1\}$ are the values assumed by u_{2s-1}, u_{2s}, and $a^{2s-1}_{m_1}, a^{2s}_{m_1} \in \{1, -1\}$ are the values assumed by $\hat{u}_{2s-1}, \hat{u}_{2s}$. Moreover, let n_1 and m_1, respectively, be the decimal numbers corresponding to the two K-length binary sequences, when those $a^k_{n_1}$ and $a^k_{m_1}$ assuming a -1 value in the sequences are reassigned a 0 value. Let Q_{n_1} denote the number of 1's in the sequence $(a^1_{n_1}, a^2_{n_1}, \ldots, a^{2s-1}_{n_1}, a^{2s}_{n_1}, \ldots, a^{2S-1}_{n_1}, a^{2S}_{n_1})$. Define $F_{n_1,m_1}, F_{n_1}, T_{n_1,m_1}, d_{n_1,m_1}$ as (18)–(21), shown at the bottom of the page.

Furthermore, let M be an integer that satisfies $(P^M_d(1-P_d)^{K-M}/P^M_f(1-P_f)^{K-M}) > (\pi_0/\pi_1)$ and $(P^{M-1}_d(1-P_d)^{K-M+1}/P^{M-1}_f(1-P_f)^{K-M+1}) < (\pi_0/\pi_1)$, i.e., M is the smallest number of nodes that can decide $\mathcal{H}_1$ while $\mathcal{H}_1$ is true and the FC decides correctly, had all communication channels been error free. Define the sets $S_0 = \{d_{n_1,m_1} \text{ where } Q_{n_1} < M\}$ and $S_1 = \{d_{n_1,m_1} \text{ where } Q_{n_1} \geq M\}$. Note that all entries of S_0 and S_1 are, respectively, negative and positive. Let $|S_0|$ and $|S_1|$ denote the cardinalities of S_0 and S_1, respectively. Utilizing the given notations, we can rewrite $f\ (z_{2s-1}, z_{2s} \text{ for } s = 1, \ldots, S|\mathcal{H}_\ell)$ in Λ as (22), shown at the bottom of the page. Since sensing noise terms are identically distributed and uncorrelated, we find $P(F_{n_1}|\mathcal{H}_\ell) = \prod_{s=1}^S P(u_{2s-1} = a^{2s-1}_{n_1}|\mathcal{H}_\ell)P(u_{2s} = a^{2s}_{n_1}|\mathcal{H}_\ell)$ in (22), and thus, $P(F_{n_1}|\mathcal{H}_1) = P^{Q_{n_1}}_d(1-P_d)^{K-Q_{n_1}}$, and $P(F_{n_1}|\mathcal{H}_0) = P^{Q_{n_1}}_f(1-P_f)^{K-Q_{n_1}}$. The term T_{n_1,m_1} in (22) is calculated using (8) and depends on the average received SNR $\bar{\gamma}_{hs}$ corresponding to internode communication. Combining (21) and (22), we find (23) and (24), shown at the bottom of the next page, where $\mathcal{T}_{e_1|h} = P(\sum_{n_1,m_1} d_{n_1,m_1} > 0|F_{n,m})$ in (23) and $\mathcal{T}_{e_2|h} = 1 - \mathcal{T}_{e_1|h}$ in (24). Note that $P_{e_1|h}$ in (23) and $P_{e_2|h}$ in (24) depend on h_{2s-1}, h_{2s} for $s = 1, \ldots, S$ only through $\mathcal{T}_{e_1|h}$ and $\mathcal{T}_{e_2|h}$, respectively. These imply that the problem of finding upper bounds on $P_{e_1|h}, P_{e_2|h}$

[8] The derivations in this section also hold true for i.i.d. sensing noise terms.

$$F_{n_1,m_1} = \left\{u_{2s-1} = a^{2s-1}_{n_1}, u_{2s} = a^{2s}_{n_1}, \hat{u}_{2s-1} = a^{2s-1}_{m_1}, \hat{u}_{2s} = a^{2s}_{m_1} \text{ for } s = 1, \ldots, S\right\} \tag{18}$$

$$F_{n_1} = \left\{u_{2s-1} = a^{2s-1}_{n_1}, u_{2s} = a^{2s}_{n_1} \text{ for } s = 1, \ldots, S\right\} \tag{19}$$

$$T_{n_1,m_1} = \prod_{s=1}^{S} P\left(\hat{u}_{2s-1} = a^{2s-1}_{m_1}|u_{2s-1} = a^{2s-1}_{n_1}\right) P\left(\hat{u}_{2s} = a^{2s}_{m_1}|u_{2s} = a^{2s}_{n_1}\right) \tag{20}$$

$$d_{n_1,m_1} = \left(\pi_1 P^{Q_{n_1}}_d(1-P_d)^{K-Q_{n_1}} - \pi_0 P^{Q_{n_1}}_f(1-P_f)^{K-Q_{n_1}}\right) \times T_{n_1,m_1} \prod_{s=1}^{S} f\left(z_{2s-1}, z_{2s}|u_{2s-1} = a^{2s-1}_{n_1}, u_{2s} = a^{2s}_{n_1}, \hat{u}_{2s-1} = a^{2s-1}_{m_1}, \hat{u}_{2s} = a^{2s}_{m_1}\right) \tag{21}$$

$$f(z_{2s-1}, z_{2s} \text{ for } s = 1, \ldots, S|\mathcal{H}_\ell) = \sum_{n_1,m_1} P(F_{n_1}|\mathcal{H}_\ell) T_{n_1,m_1} \prod_{s=1}^{S} f\left(z_{2s-1}, z_{2s}|u_{2s-1} = a^{2s-1}_{n_1}, u_{2s} = a^{2s}_{n_1}, \hat{u}_{2s-1} = a^{2s-1}_{m_1}, \hat{u}_{2s} = a^{2s}_{m_1}\right) \tag{22}$$

and their corresponding averages $\bar{P}_{e_1}, \bar{P}_{e_2}$ can be reduced to finding upper bounds on $\mathcal{T}_{e_1|h}, \mathcal{T}_{e_2|h}$ and their respective averages $\bar{\mathcal{T}}_{e_1} = \mathbb{E}\{\mathcal{T}_{e_1|h}\}, \bar{\mathcal{T}}_{e_2} = \mathbb{E}\{\mathcal{T}_{e_2|h}\}$. In the Appendix, we establish (25)–(29), shown at the bottom of the page.

The upper bound on $\bar{\mathcal{T}}_{e_2}$ depends on t. Our simulations indicate that the bound is minimized for $t \approx 0.3$. Furthermore, the upper bounds depend on the power allocation parameter α. In Section VII, we investigate the optimal α that minimizes these bounds. In the ideal case when the internode communication is error free, we find $a_n^{2s-1} = a_m^{2s-1}$ and $a_n^{2s} = a_m^{2s}$, and thus, (28) and (29), respectively, reduce to $\mathcal{D}_1(n, m, n_1, m_1) = (1 + (\alpha\bar{\gamma}_h\bar{a}_1/8))^{-2}$ and $\mathcal{D}_2(n, m, n_1, m_1) = (1 + (\alpha(t^2 - t)\bar{\gamma}_h\bar{a}_1/2))^{-2}$.

B. Classical Parallel Fusion Architecture

Leveraging on the derivations in Section VI-A, we provide upper bounds on $\bar{\mathcal{T}}_{e_1}, \bar{\mathcal{T}}_{e_2}$. In fact, the absence of internode communication renders the notations in Section VI-A simple, as the indexes m, m_1 and the decisions $\hat{u}_{2s-1}, \hat{u}_{2s}$ are dropped, z_{2s-1}, z_{2s} are substituted with y_{2s-1}, y_{2s}, and the noise terms δ_s^1, δ_s^2 are substituted with v_{2s-1}, v_{2s}. Consequently, the derivations of the upper bounds become rather easy. In particular, instead of d_{n_1,m_1} in (21), we define d_{n_1} in (30), shown at the bottom of the page. Moreover, the relationship between $P_{e_1|h}, \mathcal{T}_{e_1|h}$ in (23) and $P_{e_2|h}, \mathcal{T}_{e_2|h}$ in (24) can be revised as follows:

$$\begin{aligned} P_{e_1|h} &= \pi_0 P\left(\sum_{n_1} d_{n_1} > 0|\mathcal{H}_0\right) = \pi_0 \sum_n \mathcal{T}_{e_1|h} P(F_n|\mathcal{H}_0) \\ P_{e_2|h} &= \pi_1 P\left(\sum_{n_1} d_{n_1} < 0|\mathcal{H}_1\right) = \pi_1 \sum_n \mathcal{T}_{e_2|h} P(F_n|\mathcal{H}_1) \end{aligned} \tag{31}$$

in which F_n is defined in (19). We redefine $S_0 = \{d_{n_1},\ \text{where } Q_{n_1} < M\}$ and $S_1 = \{d_{n_1},\ \text{where } Q_{n_1} \geq M\}$,

---

$$P_{e_1|h} = \pi_0 P\left(\sum_{n_1,m_1} d_{n_1,m_1} > 0|\mathcal{H}_0\right) = \pi_0 \sum_{n,m} \mathcal{T}_{e_1|h} P(F_{n,m}|\mathcal{H}_0) = \pi_0 \sum_{n,m} \mathcal{T}_{e_1|h} P_f^{Q_n}(1 - P_f)^{K-Q_n} T_{n,m} \tag{23}$$

$$P_{e_2|h} = \pi_1 P\left(\sum_{n_1,m_1} d_{n_1,m_1} < 0|\mathcal{H}_1\right) = \pi_1 \sum_{n,m} \mathcal{T}_{e_2|h} P(F_{n,m}|\mathcal{H}_1) = \pi_1 \sum_{n,m} \mathcal{T}_{e_2|h} P_d^{Q_n}(1 - P_d)^{K-Q_n} T_{n,m} \tag{24}$$

$$\bar{\mathcal{T}}_{e_1} < \frac{\mathbf{1}_{\{Q_n<M\}}}{2\sqrt{|S_1|}} \sum_{d_{n_1,m_1}\in S_1} \left[\sqrt{G(n,m,n_1,m_1)} \prod_{s=1}^{S} \mathcal{D}_1(n,m,n_1,m_1)\right] + \mathbf{1}_{\{Q_n\geq M\}} \tag{25}$$

$$\bar{\mathcal{T}}_{e_2} < \frac{\mathbf{1}_{\{Q_n>M\}}}{|S_0|} \sum_{d_{n_1,m_1}\in S_0} \left[\min_t \left(|S_0|G(n,m,n_1,m_1)\right)^t \prod_{s=1}^{S} \mathcal{D}_2(n,m,n_1,m_1)\right] + \mathbf{1}_{\{Q_n\leq M\}} \tag{26}$$

$$G(n,m,n_1,m_1) = \frac{T_{n_1,m_1}}{T_{n,m}} \times \frac{\left(\pi_1 P_d^{Q_{n_1}}(1-P_d)^{K-Q_{n_1}} - \pi_0 P_f^{Q_{n_1}}(1-P_f)^{K-Q_{n_1}}\right)}{\left(\pi_0 P_f^{Q_n}(1-P_f)^{K-Q_n} - \pi_1 P_d^{Q_n}(1-P_d)^{K-Q_n}\right)} \tag{27}$$

$$\mathcal{D}_1(n,m,n_1,m_1) = \left(\left(1 + \frac{\alpha\bar{\gamma}_h\bar{a}_1}{8}\right)\left(1 + \frac{\alpha\bar{\gamma}_h\bar{a}_2}{8}\right) - \frac{\alpha^2\bar{\gamma}_h^2\bar{a}_3}{64}\right)^{-1} \tag{28}$$

$$\begin{aligned} \mathcal{D}_2(n,m,n_1,m_1) &= \left(\left(1 + \frac{\alpha(t^2-t)\bar{\gamma}_h\bar{a}_1}{2}\right)\left(1 + \frac{\alpha(t^2-t)\bar{\gamma}_h\bar{a}_2}{2}\right) - \frac{\alpha^2(t^2-t)^2\bar{\gamma}_h^2\bar{a}_3}{16}\right)^{-1} \\ \bar{a}_1 &= \left(a_n^{2s-1} - a_{n_1}^{2s-1}\right)^2 + \left(a_n^{2s} - a_{n_1}^{2s}\right)^2, \bar{a}_2 = \left(a_m^{2s-1} - a_{m_1}^{2s-1}\right)^2 + \left(a_m^{2s} - a_{m_1}^{2s}\right)^2 \\ \bar{a}_3 &= \left(a_n^{2s-1} - a_{n_1}^{2s-1}\right)\left(a_n^{2s} - a_{n_1}^{2s}\right) - \left(a_m^{2s-1} - a_{m_1}^{2s-1}\right)\left(a_m^{2s} - a_{m_1}^{2s}\right) \end{aligned} \tag{29}$$

$$d_{n_1} = \left(\pi_1 P_d^{Q_{n_1}}(1-P_d)^{K-Q_{n_1}} - \pi_0 P_f^{Q_{n_1}}(1-P_f)^{K-Q_{n_1}}\right) \prod_{s=1}^{S} f\left(y_{2s-1}, y_{2s}|u_{2s-1} = a_{n_1}^{2s-1}, u_{2s} = a_{n_1}^{2s}\right) \tag{30}$$

where all entries of S_0 and S_1 are, respectively, negative and positive. We have

$$\begin{aligned}
\mathcal{T}_{e_1|h} &< \frac{1}{|S_1|} \sum_{d_{n_1} \in S_1} P\left(|S_1| d_{n_1} > -d_n | F_n\right) \\
&= \frac{1}{|S_1|} \sum_{d_{n_1} \in S_1} P(\zeta(n,n_1) > -\ln(|S_1| G(n,n_1)) + I(n,n_1)) \\
\mathcal{T}_{e_2|h} &< \frac{1}{|S_0|} \sum_{d_{n_1} \in S_0} P\left(d_n < -|S_0| d_{n_1} | F_n\right) \\
&= \frac{1}{|S_0|} \sum_{d_{n_1} \in S_0} P(\zeta(n,n_1) > -\ln(|S_0| G(n,n_1)) + I(n,n_1)) \\
G(n,n_1) &= \frac{\pi_1 P_d^{Q_{n_1}} (1-P_d)^{K-Q_{n_1}} - \pi_0 P_f^{Q_{n_1}} (1-P_f)^{K-Q_{n_1}}}{\pi_0 P_f^{Q_n} (1-P_f)^{K-Q_n} - \pi_1 P_d^{Q_n} (1-P_d)^{K-Q_n}} \\
I(n,n_1) &= \sum_{s=1}^{S} \mathcal{K}_s(n,n_1), \text{ where} \\
\mathcal{K}_s(n,n_1) &= \frac{1}{\sigma_v^2} \left(\left| h_{2s-1} \left(a_{n_1}^{2s-1} - a_n^{2s-1}\right) \right|^2 + \left| h_{2s} \left(a_{n_1}^{2s} - a_n^{2s}\right) \right|^2 \right) \\
\zeta(n,n_1) &= \sum_{s=1}^{S} \theta_s(n,n_1), \text{ where} \\
\theta_s(n,n_1) &= \frac{2}{\sigma_v^2} \mathfrak{Re} \left\{ v_{2s-1} h_{2s-1} \left(a_{n_1}^{2s-1} - a_n^{2s-1}\right) \right. \\
&\qquad \left. + v_{2s} h_{2s} \left(a_{n_1}^{2s} - a_n^{2s}\right) \right\}.
\end{aligned}$$

Note that $\zeta(n, n_1)$ is a zero mean Gaussian RV with the variance $2I(n, n_1)$. Using similar techniques in Section VI-A we can establish (32)–(35), shown at the bottom of the page.

This completes our derivations for the upper bounds on $\bar{\mathcal{T}}_{e_1}, \bar{\mathcal{T}}_{e_2}$ and thus $\bar{P}_{e_1}, \bar{P}_{e_2}$. Our simulations indicate that the bound is minimized for $t \approx 0.3$.

C. Cooperative Fusion Architecture With Signal Fusion at Sensors

Leveraging on the derivations in Section VI-A and B, we provide upper bounds on $\bar{\mathcal{T}}_{e_1}, \bar{\mathcal{T}}_{e_2}$. In fact, the absence of internode communication renders the notations in Section VI-A simple, as the indexes m, m_1 and the decisions $\hat{u}_{2s-1}, \hat{u}_{2s}$ are dropped, z_{2s-1}, z_{2s} are substituted with y_{2s-1}, y_{2s}, and the noise terms δ_s^1, δ_s^2 are substituted with v_{2s-1}, v_{2s}. Thus, the derivations of the upper bounds become rather easy. In particular, instead of d_{n_1,m_1} in (21) or d_{n_1} in (30), we define d_{n_1} as (36), shown at the bottom of the page, where $P(\tilde{u}_{2s-1} = a_{n_1}^{2s-1}, \tilde{u}_{2s} = a_{n_1}^{2s} | \mathcal{H}_\ell)$ in (36) is determined in Section IV-B. In fact, this probability depends on sensing channels through threshold τ and sensing noise variance σ_w^2 as well as the average received SNR $\bar{\gamma}_{hs}$ corresponding to internode communication. Furthermore, the relationship between $P_{e_1|h}, \mathcal{T}_{e_1|h}$ in (23) and $P_{e_2|h}, \mathcal{T}_{e_2|h}$ in (24) can be revised as (31), in which $F_n = \{\tilde{u}_{2s-1} = a_n^{2s-1}, \tilde{u}_{2s} = a_n^{2s} \text{ for } s = 1, \ldots, S\}$. We also redefine $S_0 = \{d_{n_1} \text{ where } d_{n_1} < 0\}$ and $S_1 = \{d_{n_1} \text{ where } d_{n_1} \geq 0\}$, where all entries of S_0 and S_1 are, respectively, negative and positive. We have

$$\begin{aligned}
\mathcal{T}_{e_1|h} &< \frac{1}{|S_1|} \sum_{d_{n_1} \in S_1} P\left(|S_1| d_{n_1} > -d_n | F_n\right) \\
&= \frac{1}{|S_1|} \sum_{d_{n_1} \in S_1} P(\zeta(n,n_1) > -\ln(|S_1| G(n,n_1)) + I(n,n_1)) \\
\mathcal{T}_{e_2|h} &< \frac{1}{|S_0|} \sum_{d_{n_1} \in S_0} P\left(d_n < -|S_0| d_{n_1} | F_n\right) \\
&= \frac{1}{|S_0|} \sum_{d_{n_1} \in S_0} P(\zeta(n,n_1) > -\ln(|S_0| G(n,n_1)) + I(n,n_1))
\end{aligned}$$

$$\bar{\mathcal{T}}_{e_1} < \frac{\mathbf{1}_{\{Q_n < M\}}}{2\sqrt{|S_1|}} \sum_{d_{n_1} \in S_1} \left[\sqrt{G(n,n_1)} \prod_{s=1}^{S} \mathcal{D}_1(n,n_1) \right] + \mathbf{1}_{\{Q_n \geq M\}} \tag{32}$$

$$\bar{\mathcal{T}}_{e_2} < \frac{\mathbf{1}_{\{Q_n > M\}}}{|S_0|} \sum_{d_{n_1} \in S_0} \left[\min_t \left(|S_0| G(n,n_1)\right)^t \prod_{s=1}^{S} \mathcal{D}_2(n,n_1) \right] + \mathbf{1}_{\{Q_n \leq M\}} \tag{33}$$

$$\mathcal{D}_1(n,n_1) = \left(\left(1 + \frac{\bar{\gamma}_h \left| a_n^{2s-1} - a_{n_1}^{2s-1} \right|}{2} \right) \left(1 + \frac{\bar{\gamma}_h \left| a_n^{2s} - a_{n_1}^{2s} \right|}{2} \right) \right)^{-1} \tag{34}$$

$$\mathcal{D}_2(n,n_1) = \left(\left(1 + \frac{4(t^2 - t)\bar{\gamma}_h \left| a_n^{2s-1} - a_{n_1}^{2s-1} \right|}{2} \right) \left(1 + \frac{4(t^2 - t)\bar{\gamma}_h \left| a_n^{2s} - a_{n_1}^{2s} \right|}{2} \right) \right)^{-1} \tag{35}$$

$$\begin{aligned}
d_{n_1} = &\left(\pi_1 \prod_{s=1}^{S} P\left(\tilde{u}_{2s-1} = a_{n_1}^{2s-1}, \tilde{u}_{2s} = a_{n_1}^{2s} | \mathcal{H}_1\right) - \pi_0 \prod_{s=1}^{S} P\left(\tilde{u}_{2s-1} = a_{n_1}^{2s-1}, \tilde{u}_{2s} = a_{n_1}^{2s} | \mathcal{H}_0\right) \right) \\
&\times \prod_{s=1}^{S} f\left(y_{2s-1}, y_{2s} | \tilde{u}_{2s-1} = a_{n_1}^{2s-1}, \tilde{u}_{2s} = a_{n_1}^{2s}\right)
\end{aligned} \tag{36}$$

in which $G(n,n_1) = (g(n_1)/(-g(n)))$

$$g(n) = \pi_1 \prod_{s=1}^{S} P\left(\tilde{u}_{2s-1} = a_n^{2s-1}, \tilde{u}_{2s} = a_n^{2s} | \mathcal{H}_1\right) - \pi_0 \prod_{s=1}^{S} P\left(\tilde{u}_{2s-1} = a_n^{2s-1}, \tilde{u}_{2s} = a_n^{2s} | \mathcal{H}_0\right)$$

$$I(n,n_1) = \sum_{s=1}^{S} \mathcal{K}_s(n,n_1), \text{ where}$$

$$\mathcal{K}_s(n,n_1) = \frac{\alpha}{\sigma_v^2}\left(\left|h_{2s-1}\left(a_{n_1}^{2s-1} - a_n^{2s-1}\right)\right|^2 + \left|h_{2s}\left(a_{n_1}^{2s} - a_n^{2s}\right)\right|^2\right)$$

$$\zeta(n,n_1) = \sum_{s=1}^{S} \theta_s(n,n_1), \text{ where}$$

$$\theta_s(n,n_1) = \frac{2\sqrt{\alpha}}{\sigma_v^2}\mathfrak{Re}\left\{v_{2s-1}h_{2s-1}\left(a_{n_1}^{2s-1} - a_n^{2s-1}\right) + v_{2s}h_{2s}\left(a_{n_1}^{2s} - a_n^{2s}\right)\right\}.$$

Note that $\zeta(n,n_1)$ is a zero-mean Gaussian RV with variance $2I(n,n_1)$. Using similar techniques in Section VI-A and B, we can establish (37)–(40), shown at the bottom of the page.

This completes our derivations for the upper bounds on $\bar{\mathcal{T}}_{e_1}, \bar{\mathcal{T}}_{e_2}$ and, thus, $\bar{P}_{e_1}, \bar{P}_{e_2}$. Our numerical results show that the bound is minimized for $t \approx 0.3$. Furthermore, the upper bounds depend on the power allocation parameter α. In Section VII, we investigate the optimal α that minimizes these bounds.

D. Parallel Fusion Architecture With Local Threshold Changing at Sensors

Leveraging on the derivations in Section VI-A and B, we provide upper bounds on $\bar{\mathcal{T}}_{e_1}, \bar{\mathcal{T}}_{e_2}$. To capture all different values that $u_{2s-1}, u_{2s}, \bar{u}_{2s-1}, \bar{u}_{2s}$ for $s = 1,\ldots,S$ can take, we consider a $2K$-length sequence $(a_{n_1}^1, a_{n_1}^2, a_{m_1}^1, a_{m_2}^2, \ldots, a_{n_1}^{2S-1}, a_{n_1}^{2S}, a_{m_1}^{2S-1}, a_{m_1}^{2S})$, where $a_{n_1}^{2s-1}, a_{n_1}^{2s} \in \{1,-1\}$ and $a_{m_1}^{2s-1}, a_{m_1}^{2s} \in \{1,-1\}$, respectively, are the values assumed by u_{2s-1}, u_{2s} and $\bar{u}_{2s-1}, \bar{u}_{2s}$. Let $Q_{n_1,m_1}^1, Q_{n_1,m_1}^2, Q_{n_1,m_1}^3, Q_{n_1,m_1}^4$, respectively, denote the number of cases in the given sequence that $a_{n_1}^{s'} = a_{m_1}^{s'} = 1$, $a_{n_1}^{s'} = -a_{m_1}^{s'} = 1$, $a_{n_1}^{s'} = -a_{m_1}^{s'} = -1$, and $a_{n_1}^{s'} = a_{m_1}^{s'} = -1$ for $s' = 2s, 2s-1$, $s = 1,\ldots,S$. Instead of F_{n_1,m_1} in (17) and d_{n_1,m_1} in (18), we redefine them as follows:

$$F_{n_1,m_1} = \left\{u_{2s-1} = a_{n_1}^{2s-1}, u_{2s} = a_{n_1}^{2s}, \bar{u}_{2s-1} = a_{m_1}^{2s-1}, \bar{u}_{2s} = a_{m_1}^{2s} \text{ for } s = 1,\ldots,S\right\}$$

$$d_{n_1,m_1} = \left(\pi_1 \prod_{j=1}^{4} P_{d_j}^{Q_{n_1,m_1}^j} - \pi_0 \prod_{j=1}^{4} P_{f_j}^{Q_{n_1,m_1}^j}\right) \times \prod_{s=1}^{S} f\left(z_{2s-1}, z_{2s} | u_{2s-1} = a_{n_1}^{2s-1}, u_{2s} = a_{n_1}^{2s}, \bar{u}_{2s-1} = a_{m_1}^{2s-1}, \bar{u}_{2s} = a_{m_1}^{2s}\right) \quad (41)$$

where $P(\bar{u}_i = 1|u_i = -u_j = -1, \mathcal{H}_\ell) = P(x_i > \tau_1|\mathcal{H}_\ell)$, $P(\bar{u}_i = -1|u_i = -u_j = 1, \mathcal{H}_\ell) = P(\tau < x_i < \tau_1|\mathcal{H}_\ell)$, $P(\bar{u}_i = 1|u_i = -u_j = -1, \mathcal{H}_\ell) = P(\tau_2 < x_i < \tau|\mathcal{H}_\ell)$, and $P(\bar{u}_i = -1|u_i = -u_j = -1, \mathcal{H}_\ell) = P(x_i < \tau_2|\mathcal{H}_\ell)$, respectively, are equal to $P_{d_1}, P_{d_2}, P_{d_3}, P_{d_4}$ under $\mathcal{H}_1$ and are equal to $P_{f_1}, P_{f_2}, P_{f_3}, P_{f_4}$ under $\mathcal{H}_0$. Since sensing noise terms are identically distributed and uncorrelated, we find $P(F_{n_1,m_1}|\mathcal{H}_1) = \prod_{j=1}^{4} P_{d_j}^{Q_{n_1,m_1}^j}$ and $P(F_{n_1,m_1}|\mathcal{H}_0) = \prod_{j=1}^{4} P_{f_j}^{Q_{n_1,m_1}^j}$. Note that the relationship between $P_{e_1|h}, \mathcal{T}_{e_1|h}$ in (23) and $P_{e_2|h}, \mathcal{T}_{e_2|h}$ in (24) holds true. Using similar techniques in Section VI-A and B, we can establish (42)–(46), shown at the bottom of the next page.

This completes our derivations for the upper bounds on $\bar{\mathcal{T}}_{e_1}, \bar{\mathcal{T}}_{e_2}$ and, thus, $\bar{P}_{e_1}, \bar{P}_{e_2}$. The upper bound on $\bar{\mathcal{T}}_{e_2}$ depends on t. Our simulations indicate that the bound is minimized for $t \approx 0.3$.

E. Comparison of Different Schemes in Asymptotic Regime for Large S

For all four schemes discussed in Section VI-A–D, we have established the following, for large S (detailed derivations are available in [28, App. B]):

$$\bar{P}_e = \bar{P}_{e_1} + \bar{P}_{e_2} < \kappa_{l_{11}} e^{S\left(\mu_{l_{11}} + \frac{1}{2}\sigma_{l_{11}}^2\right)} + \frac{1}{2} e^{-S\frac{\mu_{l_{12}}^2}{2\sigma_{l_{12}}^2}} + \kappa_{l_{21}} e^{S\left(\mu_{l_{21}} + \frac{1}{2}\sigma_{l_{21}}^2\right)} + \frac{1}{2} e^{-S\frac{\mu_{l_{22}}^2}{2\sigma_{l_{22}}^2}}$$

where $\mu_{l_{11}} + \frac{1}{2}\sigma_{l_{11}}^2, \mu_{l_{21}} + \frac{1}{2}\sigma_{l_{21}}^2 < 0$.

$$\bar{\mathcal{T}}_{e_1} < \frac{\mathbf{1}_{\{d_n \in S_0\}}}{2\sqrt{|S_1|}} \sum_{d_{n_1} \in S_1} \left[\sqrt{G(n,n_1)} \prod_{s=1}^{S} \mathcal{D}_1(n,n_1)\right] + \mathbf{1}_{\{d_n \in S_1\}} \quad (37)$$

$$\bar{\mathcal{T}}_{e_2} < \frac{\mathbf{1}_{\{d_n \in S_1\}}}{|S_0|} \sum_{d_{n_1} \in S_1} \left[\min_t \left(|S_0| G(n,n_1)\right)^t \prod_{s=1}^{S} \mathcal{D}_2(n,n_1)\right] + \mathbf{1}_{\{d_n \in S_0\}} \quad (38)$$

$$\mathcal{D}_1(n,n_1) = \left(\left(1 + \frac{\alpha\bar{\gamma}_h\left(a_n^{2s-1} - a_{n_1}^{2s-1}\right)^2}{4}\right)\left(1 + \frac{\alpha\bar{\gamma}_h\left(a_n^{2s} - a_{n_1}^{2s}\right)^2}{4}\right)\right)^{-1} \quad (39)$$

$$\mathcal{D}_2(n,n_1) = \left(\left(1 + \alpha(t^2 - t)\bar{\gamma}_h\left(a_n^{2s-1} - a_{n_1}^{2s-1}\right)^2\right)\left(1 + \alpha(t^2 - t)\bar{\gamma}_h\left(a_n^{2s} - a_{n_1}^{2s}\right)^2\right)\right)^{-1} \quad (40)$$

Moreover, $\mu_{l_{11}}, \mu_{l_{12}}, \mu_{l_{21}}, \mu_{l_{22}}$ and $\sigma^2_{l_{11}}, \sigma^2_{l_{12}}, \sigma^2_{l_{21}}, \sigma^2_{l_{22}}$ and $\kappa_{l_{11}}, \kappa_{l_{21}}$ differ for different schemes and do not depend on S (they only depend on $\text{SNR}_h, \text{SNR}_c$ defined in Section VII and π_0). For each scheme, we examine these four exponentials and keep the dominant exponential. Let $\kappa_{l_x} e^{-S\gamma_x}$ for $x = a, b, c, d$ be the dominant exponent, respectively, for schemes discussed in Section VI-A–D, where $\gamma_x = \min\{-(\mu_{l_{11}} + (1/2)\sigma^2_{l_{11}}), (\mu^2_{l_{12}}/2\sigma_{l_{12}}), -(\mu_{l_{21}} + (1/2)\sigma^2_{l_{21}}), (\mu^2_{l_{22}}/2\sigma^2_{l_{22}})\}$, and κ_{l_x} be its corresponding multiplicative scalar. When comparing the error exponents of any pair of these four schemes, for instance, schemes in Section VI-A and B, we have $\lim_{S\to\infty}((\ln(\kappa_{l_a} e^{-S\gamma_a})/S) - (\ln(\kappa_{l_b} e^{-S\gamma_b})/S)) = \gamma_b - \gamma_a$, implying that such a difference depends on $\text{SNR}_h, \text{SNR}_c, \pi_0$ only and does not change with S. This analysis suggests that our numerical findings in Section VII on performance comparison between different schemes should not vary much for large $S = (K/2)$. In fact, our simulation results show that performance comparison between different schemes, given $\text{SNR}_h, \text{SNR}_c, \pi_0$, remains the same for $K = 10$, 14, 20 (due to space limitations, we only include the results for $K = 20$ in Table IV).

VII. Numerical Results

Here, we evaluate and compare the performance of the proposed schemes in Sections III–V, against the conventional scheme in Section II-B. For the sake of presentation, we refer to the schemes in Sections II-B, III–V, respectively, as "parallel," "STC6@sensors," and "fusion6@sensors," "threshold changing6@sensors." We consider $K = 10$ sensors ($S = 5$ groups of paired sensors). We assume that the sensing noise terms w_k are identically distributed, i.e., $\sigma^2_{w_k} = \sigma^2_w$, and $\rho_{ij} = \rho$ characterizes the correlation. We define $\text{SNR}_c = -20\log_{10}\sigma_w$ as the SNR corresponding to sensing channels. We let the distances between the sensors and the FC $d = 10$ m, the distances between the cooperative partners within each group $d_0 = 2$ m, the variance of receiver noise terms $\sigma^2_v = \sigma^2_\eta = -50$ dBm, the path-loss exponent $\varepsilon = 2$, and the antenna gain $\mathcal{G} = -30$ dB. To make a fair comparison among different schemes, we enforce the sensors in all schemes to transmit the same power $\mathcal{P}$. In "STC6@sensors" and "fusion6@sensors," a sensor spends $(1-\alpha)\mathcal{P}$ and $\alpha\mathcal{P}$, respectively, for communicating with its cooperative partner and with the FC, where α is different in these two schemes. We define $\text{SNR}_h = 10\log_{10}\bar{\gamma}_h$, in which $\bar{\gamma}_h = (\sigma^2_h/\sigma^2_v) = (P\mathcal{G}/d^\varepsilon\sigma^2_v)$. Our goal is to investigate the average error $\bar{P}_e$ of "STC6@sensors," "fusion6@sensors," and "threshold changing6@sensors" against that of "parallel," as SNR_h and SNR_c vary and identify different regimes in which these schemes outperform "parallel." Note that, in "STC6@sensors" and "fusion6@sensors," given SNR_h and SNR_c, average error $\bar{P}_e$ depends on α, i.e., one would expect that there is an optimal power allocation α^* at which $\bar{P}_e$ attains its minimum, given SNR_h and SNR_c. We start with investigating α^*.

Optimal Power Allocation When the FC Employs LRT Rule: We start with "STC6@sensors." Fig. 1(a) plots $\bar{P}_e$ versus α for $\text{SNR}_h = 5$ dB, $\text{SNR}_c = 2$, 6, 10 dB and $\pi_0 = 0.6$, assuming $\rho = 0$. We observe that $\alpha^* \approx 0.65$, regardless of the variations in SNR_c values. Fig. 1(b) plots $\bar{P}_e$ versus α for $\text{SNR}_c = 6$ dB, $\text{SNR}_h = 5$, 10, 15 dB and $\pi_0 = 0.6$, assuming $\rho = 0$. We observe that α^* increases as SNR_h (or, equivalently, $\bar{\gamma}_h$) increases; in particular, we obtain $\alpha^* \approx 0.6, 0.7, 0.8$, respectively, for $\text{SNR}_h = 5$, 10, 15 dB. These observations can be explained

$$\bar{\mathcal{T}}_{e_1} < \frac{\mathbf{1}_{\{d_{n,m}\in S_0\}}}{2\sqrt{|S_1|}} \sum_{d'_{n_1,m_1}\in S_1} \left[\sqrt{G(n,m,n_1,m_1)} \prod_{s=1}^{S} \mathcal{D}_1(n,m,n_1,m_1)\right] + \mathbf{1}_{\{d_{n,m}\in S_1\}} \tag{42}$$

$$\bar{\mathcal{T}}_{e_2} < \frac{\mathbf{1}_{\{d_{n,m}\in S_1\}}}{|S_0|} \sum_{d_{n,m}\in S_0} \left[\min_t (|S_0| G(n,m,n_1,m_1))^t \prod_{s=1}^{S} \mathcal{D}_2(n,m,n_1,m_1)\right] + \mathbf{1}_{\{d_{n,m}\in S_0\}} \tag{43}$$

$$\text{in which } S_0 = \left\{ d_{n_1,m_1} \text{ where } \frac{\prod_{j=1}^4 P_{d_j}^{Q^j_{n_1,m_1}}}{\prod_{j=1}^4 P_{f_j}^{Q^j_{n_1,m_1}}} < \frac{\pi_0}{\pi_1} \right\}, S_1 = \left\{ d_{n_1,m_1} \text{ where } \frac{\prod_{j=1}^4 P_{d_j}^{Q^j_{n_1,m_1}}}{\prod_{j=1}^4 P_{f_j}^{Q^j_{n_1,m_1}}} > \frac{\pi_0}{\pi_1} \right\}$$

$$G(n,m,n_1,m_1) = \frac{\left(\pi_1 \prod_{j=1}^4 P_{d_j}^{Q^j_{n_1,m_1}} - \pi_0 \prod_{j=1}^4 P_{f_j}^{Q^j_{n_1,m_1}}\right)}{\left(\pi_1 \prod_{j=1}^4 P_{d_j}^{Q^j_{n,m}} - \pi_0 \prod_{j=1}^4 P_{f_j}^{Q^j_{n,m}}\right)} \tag{44}$$

$$\mathcal{D}_1(n,m,n_1,m_1) = \left(\left(1 + \frac{\alpha\bar{\gamma}_h\bar{a}_1}{8}\right)\left(1 + \frac{\alpha\bar{\gamma}_h\bar{a}_2}{8}\right) - \frac{\alpha^2\bar{\gamma}_h^2\bar{a}_3}{64}\right)^{-1} \tag{45}$$

$$\mathcal{D}_2(n,m,n_1,m_1) = \left(\left(1+\frac{\alpha(t^2-t)\bar{\gamma}_h\bar{a}_1}{2}\right)\left(1+\frac{\alpha(t^2-t)\bar{\gamma}_h\bar{a}_2}{2}\right) - \frac{\alpha^2(t^2-t)^2\bar{\gamma}_h^2\bar{a}_3}{16}\right)^{-1}, \bar{a}_1 = \left(a_n^{2s-1} - a_{n_1}^{2s-1}\right)^2 + \left(a_m^{2s} - a_{m_1}^{2s}\right)^2$$

$$\bar{a}_2 = \left(a_m^{2s-1} - a_{m_1}^{2s-1}\right)^2 + \left(a_n^{2s} - a_{n_1}^{2s}\right)^2$$

$$\bar{a}_3 = \left(a_n^{2s-1} - a_{n_1}^{2s-1}\right)\left(a_m^{2s} - a_{m_1}^{2s}\right) - \left(a_m^{2s-1} - a_{m_1}^{2s-1}\right)\left(a_n^{2s} - a_{n_1}^{2s}\right) \tag{46}$$

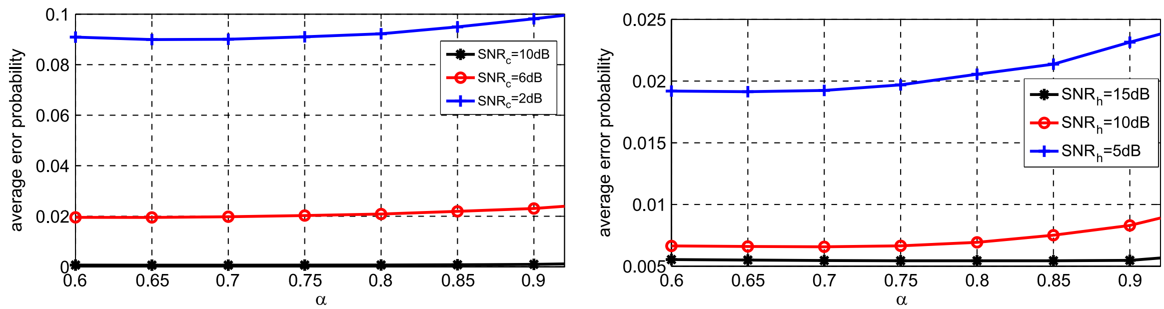

(a) (b)

Fig. 1. "STC@sensors": LRT rule. (a) $\mathrm{SNR}_h = 5$ dB with $\mathrm{SNR}_c = 2$, 6, and 10 dB. (b) $\mathrm{SNR}_c = 6$ dB with $\mathrm{SNR}_h = 5$, 10, and 15 dB.

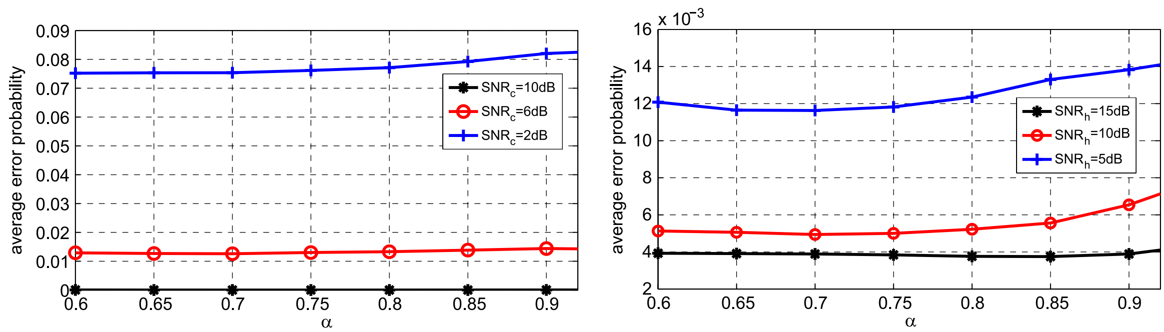

(a) (b)

Fig. 2. "fusion@sensors": LRT rule. (a) $\mathrm{SNR}_h = 5$ dB with $\mathrm{SNR}_c = 2$, 6, and 10 dB. (b) $\mathrm{SNR}_c = 6$ dB with $\mathrm{SNR}_h = 5$, 10, and 15 dB.

considering our analytical results in (23)–(29) in Section VI-A. Recall that $T_{n,m}, T_{n_1,m_1}$ in (27) capture the errors during internode communication and depend on the average received SNR $\bar{\gamma}_{hs}$ corresponding to internode communication, which, for $\sigma_\eta^2 = \sigma_v^2$, reduces to $\bar{\gamma}_{hs} = (d/d_0)^\varepsilon(1-\alpha)\bar{\gamma}_h$. This implies that $G(n,m,n_1,m_1)$ is decoupled into two fractions, where the first fraction depends on SNR_c (through the local performance indexes P_d, P_f), and the second fraction depends on $(d/d_0)^\varepsilon(1-\alpha)\bar{\gamma}_h$. On the other hand, the inverses of $\mathcal{D}_1(n,m,n_1,m_1), \mathcal{D}_2(n,m,n_1,m_1)$ depend on $\alpha\bar{\gamma}_h$ only, capturing the errors of sensor–FC communication channels. Due to this decoupling of the effective factors in the terms of $\bar{P}_e$, we expect that α^* becomes insensitive to variations of SNR_c (for fixed d, d_0, SNR_h) and varies as SNR_h changes (for fixed d, d_0, SNR_c). For the scenario where the distance between cooperative partners is shorter than the distance between the nodes and the FC, we expect $\alpha^* > 0.5$, i.e., a sensor spends a higher (lower) percentage of its transmit power for communicating with the FC (its cooperative partner). These observations are in agreement with the fact that the local information exchange in "STC6@sensors" does not affect the local error probability $p_{e_i} = P(u_i = -1|\mathcal{H}_1)\pi_1 + P(u_i = 1|\mathcal{H}_0)\pi_0$ at $\mathcal{S}_i$ (which depends on SNR_c through P_d, P_f); it rather provides a form of "decision diversity," to mitigate the fading effect during sensor–FC communication, i.e., it improves the global performance $\bar{P}_e$ at the FC via reducing the errors during intersensor and sensor–FC communication. We continue with "fusion6@sensors." Fig. 2(a) plots $\bar{P}_e$ versus α for $\mathrm{SNR}_h = 5$ dB; $\mathrm{SNR}_c = 2$, 6, and 10 dB; and $\pi_0 = 0.6$, assuming $\rho = 0$. We observe that α^* increases as SNR_c increases; in particular, we obtain $\alpha^* \approx 0.6, 0.7, 0.8$, respectively, for $\mathrm{SNR}_c = 2, 6, 10$ dB. Comparing this trend with that of "STC6@sensors" in Fig. 1(a), we notice that the schemes have different trends.

Fig. 2(b) plots $\bar{P}_e$ versus α for $\mathrm{SNR}_c = 6$ dB; $\mathrm{SNR}_h = 5$, 10, and 15 dB; and $\pi_0 = 0.6$, assuming $\rho = 0$. We observe that α^* increases as SNR_h (or, equivalently, $\bar{\gamma}_h$) increases; in particular, we obtain $\alpha^* \approx 0.7$, 0.7, and 0.85, respectively, for $\mathrm{SNR}_h = 5$, 10, and 15 dB. Comparing this trend with that of "STC6@sensors" in Fig. 1(b), we observe that the schemes have similar trends. These observations can be explained considering our analytical results in (37) and (38) in Section VI-C. Note that similar to "STC6@sensors," the inverses of $\mathcal{D}_1(n,n_1), \mathcal{D}_2(n,n_1)$ depend on $\alpha\bar{\gamma}_h$ only, capturing the errors of sensor–FC communication channels. However, the structure of $G(n,n_1)$ is different from that of $G(n,m,n_1,m_1)$ in "STC6@sensors." In particular, examining $G(n,n_1)$ reveals that this term depends on $P(\tilde{u}_{2s-1}, \tilde{u}_{2s}$ for all pairs$|\mathcal{H}_\ell)$ given in (12), which, as we have previously mentioned in Section IV-B, depends on SNR_c (through P_d, P_f) as well as the average received SNR $\bar{\gamma}_{hs}$ corresponding to internode communication. This implies that, different from $G(n,m,n_1,m_1)$ in "STC6@sensors," the impacts of effective factors SNR_c and $(d/d_0)^\varepsilon(1-\alpha)\bar{\gamma}_h$ in $G(n,n_1)$ cannot be decoupled, and hence, α^* varies as SNR_c changes (for fixed d, d_0, SNR_h) or SNR_h changes (for fixed d, d_0, SNR_c). These observations are in agreement with the fact that the local information exchange in "fusion6@sensors," different from "STC6@sensors," affects the the local error probability $p_{e_i} = P(\tilde{u}_i = -1|\mathcal{H}_1)\pi_1 + P(\tilde{u}_i = 1|\mathcal{H}_0)\pi_0$ at $\mathcal{S}_i$. Therefore, it improves the global performance $\bar{P}_e$ at the FC via improving the local error probability

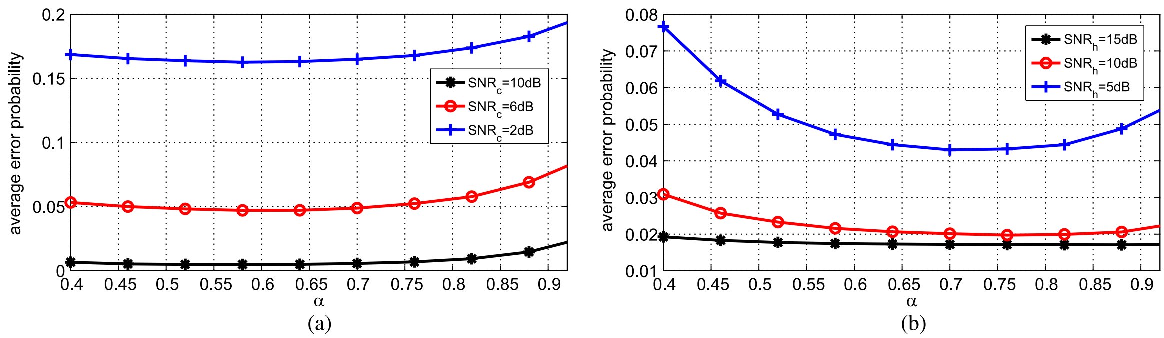

Fig. 3. "STC@sensors": majority rule. (a) $\mathrm{SNR}_h = 5$ dB with $\mathrm{SNR}_c = 2$, 6, and 10 dB. (b) $\mathrm{SNR}_c = 6$ dB with $\mathrm{SNR}_h = 5$, 10, and 15 dB.

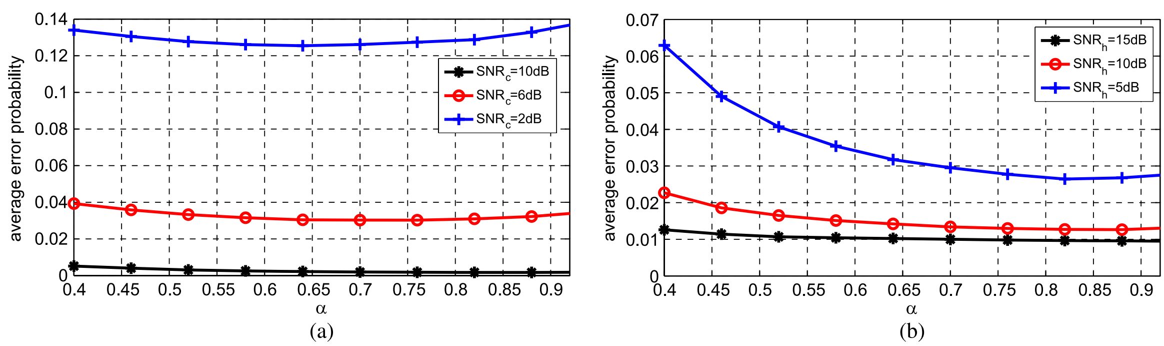

Fig. 4. "fusion@sensors": majority rule. (a) $\mathrm{SNR}_h = 5$ dB with $\mathrm{SNR}_c = 2$, 6, and 10 dB. (b) $\mathrm{SNR}_c = 6$ dB with $\mathrm{SNR}_h = 5$, 10, and 15 dB.

at the sensors. As SNR_c decreases (for fixed d, d_0, SNR_h), the reliability of the initial decision u_i at $\mathcal{S}_i$ (which is based on observation x_i) reduces, and hence, the local information exchange is more needed to form the new decision $\tilde{u}_i$ with higher reliability, where more local information exchange is translated into a higher (lower) percentage of transmit power for internode communication (sensor–FC communication) or, equivalently, smaller α^*.

Optimal Power Allocation When the FC Employs Majority Rule: Similar observations are made when the FC employs the majority rule. Figs. 3(a) and 4(a), respectively, plot $\bar{P}_e$ versus α, for "STC6@sensors" and "fusion6@sensors," when $\mathrm{SNR}_h = 5$ dB, $\mathrm{SNR}_c = 2$, 6, and 10 dB, and $\pi_0 = 0.6$. Figs. 3(b) and 4(b), respectively, plot $\bar{P}_e$ versus α, for "STC6@sensors" and "fusion6@sensors," when $\mathrm{SNR}_c = 6$ dB, $\mathrm{SNR}_h = 5$, 10, and 15 dB, and $\pi_0 = 0.6$. Comparing Fig. 1(a) with Fig. 3(a), Fig. 2(a) with Fig. 4(a), Fig. 1(b) with Fig. 3(b), and Fig. 2(b) with Fig. 4(b), we can make similar observations regarding the variations of α^* as SNR_c or SNR_h changes. For each scheme, when we compare the value of α^* for LRT and majority rules, given $d, d_0, \mathrm{SNR}_c, \mathrm{SNR}_h$, we find that α^* corresponding to the majority rule is larger than that of the LRT rule, i.e., a sensor spends a higher (lower) percentage of its transmit power for communicating with the FC (its cooperative partner). This is due to the fact that the majority rule demodulates first the sensor–FC channel outputs to find the channel inputs, rather than using the channel outputs directly for fusion, resembling the concept of "hard versus soft decoding" in [23]. To compensate for the information loss due to demodulation and its negative impact on error, each sensor is required to invest a higher percentage of its transmit power for communicating with the FC.

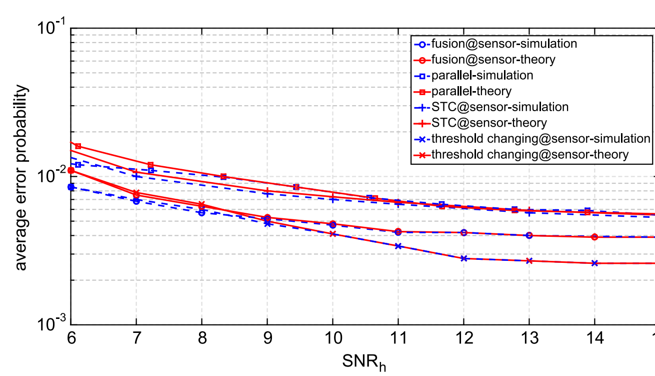

Fig. 5. Monte Carlo simulation versus analytical results.

Performance Comparison of Different Schemes: To validate our performance analysis in Section VI, Fig. 5 shows $\bar{P}_e$ of "parallel," "STC6@sensors," "fusion6@sensors," and "threshold changing6@sensors" versus SNR_h for $\mathrm{SNR}_c = 6$ dB and $\pi_0 = 0.6$, to compare the analytical and Monte Carlo simulation results. We obtain $\bar{P}_e$ of "STC6@sensors" and "fusion6@sensors," using α^* corresponding to SNR_h and SNR_c values. The figure demonstrates a good agreement between theory and simulation. It also shows that, different from conventional communication systems, $\bar{P}_e$ has an error floor at high SNR_h. This behavior is due to the fact that $\bar{P}_e$ in our distributed detection system is dependent on SNR_h and SNR_c.

TABLE I
ALL SCHEMES, LRT RULE, $\rho = 0$, $K = 10$

	$\mathrm{SNR}_c = 10\mathrm{dB}$			$\mathrm{SNR}_c = 6\mathrm{dB}$			$\mathrm{SNR}_c = 2\mathrm{dB}$			
SNR_h	5dB	10dB	15dB	5dB	10dB	15dB	5dB	10dB	15dB	
parallel	$1.9e{-4}$	$3.8e{-5}$	$2.0e{-5}$	$1.2e{-2}$	$7.3e{-3}$	$5.6e{-3}$	$7.6e{-2}$	$6.6e{-2}$	$6.4e{-2}$	$\pi_0 = 0.6$
STC	$8.7e{-4}$	$3.1e{-5}$	$1.4e{-5}$	$1.8e{-2}$	$6.9e{-3}$	$5.4e{-3}$	$8.9e{-2}$	$6.5e{-2}$	$6.3e{-2}$	
fusion	$1.9e{-4}$	$1.7e{-5}$	$1.4e{-5}$	$1.2e{-2}$	$4.8e{-3}$	$3.9e{-3}$	$7.4e{-2}$	$5.5e{-2}$	$5.2e{-2}$	
threshold	$3.4e{-4}$	$1.7e{-5}$	$3.0e{-6}$	$1.2e{-2}$	$4.4e{-3}$	$2.6e{-3}$	$7.5e{-2}$	$4.7e{-2}$	$3.7e{-2}$	
parallel	$3.0e{-4}$	$4.3e{-5}$	$2.3e{-5}$	$1.3e{-2}$	$7.4e{-3}$	$6.7e{-3}$	$8.1e{-2}$	$7.0e{-2}$	$6.6e{-2}$	$\pi_0 = 0.7$
STC	$8.9e{-4}$	$2.9e{-5}$	$1.9e{-5}$	$1.9e{-2}$	$7.1e{-3}$	$6.2e{-3}$	$9.4e{-2}$	$6.9e{-2}$	$6.5e{-2}$	
fusion	$2.3e{-4}$	$2.0e{-5}$	$7e{-6}$	$1.3e{-2}$	$5.9e{-3}$	$5.4e{-3}$	$7.9e{-2}$	$5.9e{-2}$	$5.5e{-2}$	
threshold	$3.9e{-4}$	$1.5e{-5}$	$0.0e{-6}$	$1.2e{-2}$	$3.9e{-3}$	$2.4e{-3}$	$7.1e{-2}$	$4.6e{-2}$	$3.5e{-2}$	

In fact, had all communication channels been error free, $\bar{P}_e$ of "parallel" would be

$$\begin{aligned}\bar{P}_e &= \pi_1 P\left(\frac{P_d^n(1-P_d)^{2S-n}}{P_f^n(1-P_f)^{2S-n}} < \frac{\pi_0}{\pi_1}\right)\\ &\quad + \pi_0 P\left(\frac{P_d^n(1-P_d)^{2S-n}}{P_f^n(1-P_f)^{2S-n}} > \frac{\pi_0}{\pi_1}\right)\\ &= \pi_1 \sum_{n=0}^{M-1} \frac{(2S)!}{(2S-n)!n!} P_d^n(1-P_d)^{2S-n}\\ &\quad + \pi_0 \sum_{n=M}^{2S} \frac{(2S)!}{(2S-n)!n!} P_f^n(1-P_f)^{2S-n} \qquad (47)\end{aligned}$$

where M satisfies $(P_d^M(1-P_d)^{2S-M}/P_f^M(1-P_f)^{2S-M}) > (\pi_0/\pi_1)$. Equation (47) indicates that the error floor depends on SNR_c (through P_d, P_f), and as SNR_c reduces, the error floor increases. Fig. 5 also shows that "parallel" and "STC6@sensors" have similar error floors, whereas "fusion6@sensors" have a lower error floor. These observations are in agreement with the fact that the local information exchange in "STC6@sensors" improves $\bar{P}_e$ via providing "decision diversity," without changing the local error probability at $\mathcal{S}_i$ (which depends on the reliability of u_i). On the other hand, the local information exchange in "fusion6@sensors" improves $\bar{P}_e$ via improving the local error probability at $\mathcal{S}_i$ (which depends on the reliability of $\tilde{u}_i$). For moderate/high SNR_h, where the errors during intersensor and sensor–FC communication are negligible, $\bar{P}_e$ is governed by the local error probability at $\mathcal{S}_i$. Since the reliability of local decisions in "parallel" and "STC6@sensors" is identical and the reliability of local decisions in "fusion6@sensors" exceeds that of "parallel" and "STC6@sensors," we expect that "parallel" and "STC6@sensors" have similar error floors, whereas "fusion6@sensors" reach a lower error floor, and Fig. 5 confirms these. Table I tabulates $\bar{P}_e$ of "parallel," "STC6@sensors," "fusion6@sensors," and "threshold changing6@sensors," as SNR_h and SNR_c vary, for $\pi_0 = 0.6$ and $\rho = 0$, when the FC employs the LRT rule. To have a fair comparison among different schemes, we obtain $\bar{P}_e$ of "STC6@sensors" and "fusion6@sensors," using α^* corresponding to SNR_h and SNR_c values. Comparing "STC6@sensors" and "parallel," we note that for moderate SNR_h and moderate/high SNR_c, "STC@sensors" outperform "parallel," whereas the performance gain of "STC@sensors" decreases as SNR_c reduces. On the other hand, for low SNR_h, "STC@sensors" perform worse than "parallel," whereas for high SNR_h, "parallel" and "STC@sensors" reach similar error floors. These observations agree with the fact that the local information exchange in "STC@sensors" improves $\bar{P}_e$ via providing "decision diversity," without changing the local error probability at $\mathcal{S}_i$ (which depends on SNR_c). For moderate/high SNR_h, the errors during intersensor and sensor–FC communication are small, and $\bar{P}_e$ is mainly determined by SNR_c. Therefore, lowering SNR_c increases $\bar{P}_e$. On the other hand, for low SNR_h, the errors during intersensor communication negatively impact the diversity gain of "STC@sensors." Comparing "fusion@sensors" and "parallel," we note that for low SNR_h, they have similar performance, whereas for moderate/high SNR_h, "fusion@sensors" outperform "parallel" (regardless of SNR_c). In particular, for high SNR_h, the error floor of "fusion@sensors" is smaller than that of "parallel." These observations agree with the fact that for moderate/high SNR_h, $\bar{P}_e$ is dominated by the local probability error at $\mathcal{S}_i$ and that the local probability error of "fusion@sensors" is smaller than that of "parallel." Comparing "threshold changing@sensors" and "parallel," we note that the local decisions in "threshold changing@sensors" have enhanced reliability, which is due to the fact that $u_i, \bar{u}_i$ at $\mathcal{S}_i$ are obtained based on comparing the sensor's observation x_i with three thresholds (instead of one). For moderate/high SNR_h, "threshold changing@sensors" outperform "parallel" (regardless of SNR_c). This observation can be explained as follows. In this SNR_h regime, $\bar{P}_e$ is dominated by the local probability error at $\mathcal{S}_i$. Since the reliability of local decisions in "threshold changing@sensors" exceeds that of local decisions in "parallel," we expect that "threshold changing@sensors" outperform "parallel." Furthermore, "threshold changing@sensors" improve $\bar{P}_e$ over "parallel," via providing "decision diversity" through Alamouti's STC. For low SNR_h, "threshold changing@sensors" outperform "parallel" only for low SNR_c. This is because in this regime, two factors contribute to $\bar{P}_e$: unreliable local decisions and communication channel errors. Since "threshold changing@sensors" increase the reliability of local decisions, its performance exceeds that of "parallel." On the other hand, for low SNR_h and moderate/high SNR_c, where the communication channel errors are the major contributors to $\bar{P}_e$, Alamouti's STC introduces destructive signal interference and degrades the performance of "threshold changing@sensors" with respect to "parallel."

Table I also tabulates $\bar{P}_e$ of "parallel," "STC@sensors," "fusion@sensors," and "threshold changing@sensors," as SNR_h and SNR_c vary, for $\pi_0 = 0.7$ and $\rho = 0$, when the FC

TABLE II
ALL SCHEMES, MAJORITY RULE, $\rho = 0$, $K = 10$

	$\text{SNR}_c = 13$dB		$\text{SNR}_c = 10$dB			$\text{SNR}_c = 6$dB			$\text{SNR}_c = 2$dB			
SNR_h	5dB	10dB	5dB	10dB	15dB	5dB	10dB	15dB	5dB	10dB	15dB	
parallel	$2.4e{-4}$	$4e{-6}$	$1.3e{-3}$	$4.0e{-4}$	$9.0e{-5}$	$3.2e{-2}$	$2.2e{-2}$	$1.8e{-2}$	$1.4e{-1}$	$1.3e{-1}$	$1.3e{-1}$	$\pi_0 = 0.6$
STC	$1.4e{-3}$	$2e{-6}$	$4.2e{-3}$	$2.3e{-4}$	$6.0e{-5}$	$4.4e{-2}$	$2.0e{-2}$	$1.7e{-2}$	$1.5e{-1}$	$1.3e{-1}$	$1.3e{-1}$	
fusion	$1.7e{-4}$	$3e{-6}$	$1.3e{-3}$	$4.0e{-5}$	$3e{-5}$	$2.7e{-2}$	$1.3e{-2}$	$1.0e{-2}$	$1.2e{-1}$	$9.7e{-2}$	$9.0e{-2}$	
threshold			$2.4e{-2}$	$1.3e{-2}$	$1.1e{-3}$	$1.2e{-1}$	$1.0e{-1}$	$9.7e{-2}$	$2.3e{-1}$	$2.2e{-1}$	$2.1e{-1}$	
parallel			$2.0e{-3}$	$5.3e{-4}$	$2.0e{-4}$	$6.1e{-2}$	$4.2e{-2}$	$3.7e{-2}$	$2.0e{-1}$	$2.0e{-1}$	$2.0e{-1}$	$\pi_0 = 0.7$
STC			$4.9e{-3}$	$4.7e{-4}$	$1.6e{-5}$	$6.8e{-2}$	$3.9e{-2}$	$3.6e{-2}$	$1.9e{-1}$	$2.0e{-1}$	$2.0e{-1}$	
fusion			$1.2e{-3}$	$1.8e{-4}$	$6e{-5}$	$2.3e{-2}$	$1.4e{-2}$	$1.2e{-2}$	$9.2e{-2}$	$1.0e{-1}$	$9.8e{-2}$	
threshold			$2.2e{-2}$	$1.3e{-2}$	$1.0e{-3}$	$1.0e{-1}$	$9.6e{-2}$	$9.0e{-2}$	$2.0e{-1}$	$1.9e{-1}$	$1.9e{-1}$	

TABLE III
ALL SCHEMES, LRT RULE, $\pi_0 = 0.7$, $K = 10$

	$\text{SNR}_c = 10$dB			$\text{SNR}_c = 6$dB			$\text{SNR}_c = 2$dB			
SNR_h	5dB	10dB	15dB	5dB	10dB	15dB	5dB	10dB	15dB	
parallel	$7.4e{-4}$	$5.3e{-4}$	$3.8e{-4}$	$2.8e{-2}$	$2.4e{-2}$	$2.2e{-2}$	$1.10e{-1}$	$1.02e{-1}$	$9.95e{-2}$	$\rho = 0.1$
STC	$7.7e{-4}$	$4.3e{-4}$	$3.8e{-4}$	$3.2e{-2}$	$1.8e{-2}$	$2.0e{-2}$	$1.18e{-1}$	$1.02e{-1}$	$9.89e{-2}$	
fusion	$6.9e{-4}$	$3.0e{-4}$	$2.2e{-4}$	$2.5e{-2}$	$1.7e{-2}$	$1.6e{-2}$	$1.05e{-1}$	$9.5e{-2}$	$9.06e{-2}$	
threshold	$9.3e{-4}$	$2.2e{-4}$	$1.5e{-4}$	$2.6e{-2}$	$1.5e{-2}$	$1.3e{-2}$	$1.09e{-1}$	$8.7e{-2}$	$7.81e{-2}$	
parallel	$2.7e{-3}$	$1.9e{-3}$	$1.7e{-3}$	$4.0e{-2}$	$3.6e{-2}$	$3.5e{-2}$	$1.38e{-1}$	$1.32e{-1}$	$1.31e{-1}$	$\rho = 0.2$
STC	$3.4e{-3}$	$1.8e{-3}$	$1.6e{-3}$	$4.4e{-2}$	$3.5e{-2}$	$3.5e{-3}$	$1.43e{-1}$	$1.32e{-1}$	$1.32e{-1}$	
fusion	$2.5e{-3}$	$1.3e{-3}$	$1.1e{-3}$	$3.9e{-2}$	$3.3e{-2}$	$3.3e{-2}$	$1.37e{-1}$	$1.29e{-1}$	$1.25e{-1}$	
threshold	$3.1e{-2}$	$1.4e{-3}$	$1.0e{-3}$	$4.3e{-2}$	$3.4e{-2}$	$3.0e{-2}$	$1.42e{-1}$	$1.29e{-1}$	$1.24e{-1}$	
parallel	$4.8e{-3}$	$3.8e{-3}$	$3.5e{-3}$	$5.7e{-2}$	$5.2e{-2}$	$5.2e{-2}$	$1.60e{-1}$	$1.54e{-1}$	$1.54e{-1}$	$\rho = 0.3$
STC	$5.8e{-3}$	$3.5e{-3}$	$3.5e{-3}$	$6.0e{-2}$	$5.2e{-2}$	$5.1e{-3}$	$1.64e{-1}$	$1.56e{-1}$	$1.56e{-1}$	
fusion	$4.8e{-3}$	$3.4e{-3}$	$3.3e{-3}$	$5.6e{-2}$	$5.0e{-2}$	$4.9e{-2}$	$1.60e{-1}$	$1.52e{-1}$	$1.52e{-1}$	
threshold	$3.1e{-2}$	$3.5e{-3}$	$2.7e{-3}$	$6.1e{-2}$	$5.1e{-2}$	$4.9e{-2}$	$1.62e{-1}$	$1.54e{-1}$	$1.50e{-1}$	
parallel	$1.4e{-2}$	$1.4e{-2}$	$1.3e{-2}$	$9.19e{-2}$	$8.95e{-2}$	$8.99e{-2}$	$1.80e{-1}$	$1.77e{-1}$	$1.77e{-1}$	$\rho = 0.5$
STC	$1.6e{-2}$	$1.3e{-2}$	$1.3e{-2}$	$9.35e{-2}$	$8.97e{-2}$	$8.89e{-2}$	$1.79e{-1}$	$1.71e{-1}$	$1.71e{-1}$	
fusion	$1.4e{-3}$	$1.2e{-2}$	$1.2e{-2}$	$9.12e{-2}$	$8.79e{-2}$	$8.55e{-2}$	$1.72e{-1}$	$1.71e{-1}$	$1.71e{-1}$	
threshold	$1.4e{-2}$	$1.3e{-2}$	$1.0e{-2}$	$9.19e{-2}$	$8.80e{-2}$	$8.70e{-2}$	$1.80e{-1}$	$1.78e{-1}$	$1.77e{-1}$	
parallel	$3.1e{-2}$	$3.0e{-2}$	$2.9e{-2}$	$1.25e{-1}$	$1.25e{-1}$	$1.25e{-1}$	$2.10e{-1}$	$2.10e{-1}$	$2.09e{-1}$	$\rho = 0.8$
STC	$3.0e{-2}$	$2.8e{-2}$	$2.8e{-2}$	$1.25e{-1}$	$1.25e{-1}$	$1.25e{-1}$	$2.12e{-1}$	$2.09e{-1}$	$2.09e{-1}$	
fusion	$2.9e{-2}$	$2.9e{-2}$	$2.8e{-2}$	$1.25e{-1}$	$1.25e{-1}$	$1.25e{-1}$	$2.09e{-1}$	$2.09e{-1}$	$2.09e{-1}$	
threshold	$3.0e{-2}$	$3.0e{-2}$	$3.0e{-2}$	$1.29e{-1}$	$1.29e{-1}$	$1.29e{-1}$	$2.17e{-1}$	$2.20e{-1}$	$2.22e{-1}$	

employs the LRT rule. Similar observations can be made as we compare "STC@sensors" and "fusion@sensors" against "parallel" for different SNR_h and SNR_c regimes, regardless of π_0. However, when comparing "threshold changing@sensors" against "parallel" in low SNR_h, we note that the behavior changes as π_0 increases. In particular, for low SNR_h, "threshold changing@sensors" outperform "parallel" for low SNR_c when π_0 is smaller. As π_0 increases, "threshold changing@sensors" outperform "parallel" for low/moderate SNR_c, i.e., for low SNR_h, the range of SNR_c values over which "threshold changing@sensors" outperform "parallel" expands as π_0 increases. Overall, Table I indicates that for low SNR_h and moderate/high SNR_c, the proposed schemes do not have an advantage over "parallel." The exception is when π_0 is large enough ($\pi_0 \geq 0.7$), in which case "threshold changing@sensors" outperform "parallel." On the other hand, for low SNR_h and low SNR_c, "fusion@sensors" and "threshold changing@sensors" outperform "parallel." For moderate/high SNR_h, regardless of SNR_c, the schemes ranked from lowest to highest $\bar{P}_e$ are "threshold changing@sensors," "fusion@sensors," "STC@sensors," and "parallel." Table II is similar to Table I, with the difference that the FC employs the majority rule. Comparing each of the schemes "STC@sensors," "fusion@sensors," and "threshold changing@sensors" against "parallel" for different SNR_h and SNR_c regimes, we observe similar trends for the majority and LRT rules. However, when we compare the schemes to rank them based on their $\bar{P}_e$, we note the differences. In particular, for very high SNR_c, "STC@sensors" outperform all the schemes, for high SNR_c, none of the proposed schemes have an advantage over "parallel," and for moderate/low SNR_c, "fusion@sensors" outperform all the schemes.

Impact of Correlation on Performance Comparison: Table III tabulates $\bar{P}_e$ of "parallel," "STC@sensors," "fusion@sensors," and "threshold changing@sensors," as SNR_h and SNR_c vary, for $\pi_0 = 0.7$ and $\rho = 0.1$, 0.2, 0.3, 0.5, 0.8, when the FC employs the LRT rule. We observe that as ρ increases, the performance gap between the proposed schemes and "parallel" reduces. This observation can be explained as follows. As we have previously mentioned, the performance advantage of "fusion@sensors" and "threshold changing@sensors" over "parallel," when the FC employs the LRT rules, is mainly due to the fact that the local information exchange in "fusion@sensors" or the three-threshold-based test at the sensors in "threshold changing@sensors" would enhance the reliability of the local decisions (compared with "parallel") when Gaussian sensing noise terms are uncorrelated. As these noise terms become correlated and ρ increases, the increase in the reliability of the local decisions in "fusion@sensors" and "threshold changing@sensors" diminishes, and thus, these two schemes start to lose their performance gain over "parallel." For $\rho \leq 0.2$, the observations made on the performance comparison among these schemes remain the

TABLE IV
ALL SCHEMES, LRT RULE, $\rho = 0$, $\pi_0 = 0.6$, $K = 20$

	$\text{SNR}_c = 10\text{dB}$			$\text{SNR}_c = 6\text{dB}$			$\text{SNR}_c = 2\text{dB}$		
SNR_h	5dB	10dB	15dB	5dB	10dB	15dB	5dB	10dB	15dB
parallel	$3.8e{-7}$	$4.0e{-8}$	$3.0e{-9}$	$7.6e{-4}$	$3.3e{-4}$	$2.3e{-4}$	$2.3e{-2}$	$1.6e{-2}$	$1.5e{-2}$
STC	$3.8e{-6}$	$2.0e{-8}$	$2.0e{-9}$	$1.6e{-3}$	$2.6e{-4}$	$1.8e{-4}$	$2.7e{-2}$	$1.5e{-2}$	$1.3e{-2}$
fusion	$3.6e{-7}$	$5.7e{-9}$	$2.0e{-9}$	$6.0e{-4}$	$1.7e{-4}$	$9.5e{-5}$	$2.1e{-2}$	$1.3e{-2}$	$1.1e{-2}$
threshold	$8.5e{-7}$	$6.0e{-9}$	$1.0e{-10}$	$7.3e{-4}$	$1.1e{-4}$	$3.8e{-5}$	$2.1e{-2}$	$9.1e{-3}$	$6.0e{-3}$

TABLE V
ALL SCHEMES FOR A GROUP OF FOUR SENSORS, LRT RULE, $\rho = 0$, $K = 4$

	$\text{SNR}_c = 10\text{dB}$			$\text{SNR}_c = 6\text{dB}$			$\text{SNR}_c = 2\text{dB}$			
SNR_h	5dB	10dB	15dB	5dB	10dB	15dB	5dB	10dB	15dB	
parallel	$1.3e{-2}$	$5.9e{-3}$	$5.3e{-3}$	$7.3e{-2}$	$5.8e{-2}$	$5.6e{-2}$	$1.8e{-1}$	$1.5e{-1}$	$1.5e{-1}$	$\pi_0 = 0.6$
STC4	$6.1e{-2}$	$6.7e{-3}$	$5.1e{-3}$	$1.3e{-1}$	$6.0e{-2}$	$5.4e{-2}$	$1.5e{-1}$	$1.5e{-1}$	$1.5e{-1}$	
fusion4	$1.3e{-2}$	$2.8e{-3}$	$1.6e{-3}$	$7.8e{-2}$	$4.5e{-2}$	$3.7e{-2}$	$1.8e{-1}$	$1.4e{-1}$	$1.3e{-1}$	
threshold4	$2.8e{-1}$	$2.4e{-1}$	$2.0e{-1}$	$3.0e{-1}$	$2.7e{-1}$	$1.9e{-1}$	$3.9e{-1}$	$3.0e{-1}$	$2.2e{-1}$	
STC	$2.1e{-2}$	$5.8e{-3}$	$5.1e{-3}$	$8.8e{-2}$	$5.7e{-2}$	$5.4e{-2}$	$1.9e{-1}$	$1.5e{-1}$	$1.5e{-1}$	
fusion	$1.3e{-2}$	$3.8e{-3}$	$3.6e{-3}$	$7.4e{-2}$	$5.2e{-2}$	$4.9e{-2}$	$1.8e{-1}$	$1.5e{-1}$	$1.4e{-1}$	
threshold	$1.5e{-2}$	$2.8e{-3}$	$1.5e{-3}$	$7.8e{-2}$	$4.4e{-2}$	$3.5e{-2}$	$1.7e{-1}$	$1.3e{-1}$	$1.2e{-1}$	
parallel	$1.0e{-2}$	$5.5e{-3}$	$4.8e{-3}$	$6.7e{-2}$	$5.3e{-2}$	$5.0e{-2}$	$1.6e{-1}$	$1.5e{-1}$	$1.4e{-1}$	$\pi_0 = 0.7$
STC4	$5.7e{-2}$	$8.3e{-3}$	$3.5e{-3}$	$1.3e{-1}$	$5.8e{-2}$	$4.2e{-2}$	$2.0e{-1}$	$1.5e{-1}$	$1.4e{-1}$	
fusion4	$1.5e{-2}$	$4.5e{-3}$	$2.6e{-3}$	$8.2e{-2}$	$5.0e{-2}$	$4.4e{-2}$	$1.7e{-1}$	$1.4e{-1}$	$1.3e{-1}$	
threshold4	$2.3e{-1}$	$1.7e{-1}$	$2.0e{-1}$	$1.4e{-1}$	$2.0e{-1}$	$1.4e{-1}$	$2.9e{-1}$	$2.7e{-1}$	$1.2e{-1}$	
STC	$1.8e{-2}$	$5.0e{-3}$	$4.1e{-3}$	$7.9e{-2}$	$5.0e{-2}$	$4.8e{-2}$	$1.7e{-1}$	$1.4e{-1}$	$1.4e{-1}$	
fusion	$9.7e{-3}$	$4.6e{-3}$	$3.8e{-3}$	$6.7e{-2}$	$5.3e{-2}$	$4.7e{-2}$	$1.6e{-1}$	$1.4e{-1}$	$1.4e{-1}$	
threshold	$1.2e{-2}$	$3.1e{-3}$	$2.2e{-3}$	$7.0e{-2}$	$4.5e{-2}$	$3.4e{-2}$	$1.6e{-1}$	$1.3e{-1}$	$1.2e{-1}$	

same as $\rho = 0$. When ρ varies between 0.2 and 0.3, "threshold changing@sensors" outperform others for high SNR_h, "fusion@sensors" outperform others for medium SNR_h, and "parallel" and "fusion@sensors" outperform others for low SNR_h (all regardless of SNR_c). When $\rho = 0.5$ for high SNR_h and high SNR_c, "threshold changing@sensors" outperform others. For high SNR_h and medium/low SNR_c and for medium SNR_h (regardless of SNR_c), "fusion@sensors" outperform others. For low SNR_h (regardless of SNR_c), "parallel" and "fusion@sensors" outperform others. When $\rho = 0.8$, "threshold changing@sensors" have an inferior performance, regardless of SNR_h and SNR_c. Table III also shows that the performance degradation of "threshold changing@sensors" is pronounced, as ρ increases, compared with other schemes. Note that at $\rho = 0$, "threshold changing@sensors" have the lowest error floor, whereas at $\rho = 1$, all schemes have the same error floor. These imply that the rate of performance degradation of "threshold changing@sensors" must be higher than other schemes.

Impact of Increasing K: Table IV tabulates $\bar{P}_e$ of "parallel," "STC@sensors," "fusion@sensors," and "threshold changing@sensors," as SNR_h and SNR_c vary, for $\pi_0 = 0.6$, $\rho = 0$, and $K = 20$, when the FC employs the LRT rule. The observations made on the comparison between these schemes for $K = 10$ and 14 remain true.

Discussion on Increasing Number of Cooperative Partners in a Group: To investigate how the increasing number of partners impacts the performance, we consider a network of $K = 4$ sensors. Suppose sensors are positioned on the circumference of a circle on the $x-y$ plane, whose center is located at the origin and its diameter is $2\sqrt{2}$ m, and $\mathcal{S}_i$ is equally distant from $\mathcal{S}_j$ and $\mathcal{S}_k$ such that $d_{ij} = d_{ik} = 2$ m, and $d_{jk} = 2\sqrt{2}$ m. Moreover, the FC is located above the origin (above the $x-y$ plane), such that all sensors are at equal distance of $d = 10$ m from the FC. Let "STC4@sensors," "fusion4@sensors," and "threshold changing4@sensors," respectively, refer to schemes 1)–3) with four partners in one group and "STC@sensors," "fusion@sensors," and "threshold changing@sensors," respectively, refer to schemes 1)–3) with two partners in one group (two groups in the network). Table V tabulates $\bar{P}_e$ of all schemes as SNR_h and SNR_c vary, for $\pi_0 = 0.6$, 0.7 and $\rho = 0$, when the FC employs the LRT rule. Comparing all these schemes, we observe that for low SNR_h, either "parallel" or "threshold changing@sensors" outperform others (depending on SNR_c), whereas for moderate/high SNR_h, "threshold changing@sensors" outperform others, including "fusion4@sensors." These observations suggest that no performance gain is achieved as the number of cooperative partners increases beyond two. In the following, we provide our intuitive reasoning on how we expect schemes 1)–3) to perform, as the number of cooperative partners in a group increases, assuming K and sensor placements are fixed. Going from "STC@sensors" to "STC4@sensors," for fixed transmit power per sensor $\mathcal{P}$, we expect that the power consumption for intersensor communication $(1-\alpha)\mathcal{P}$ increases, as the average distances between sensors within a group increase. This leaves a sensor with smaller power, i.e., smaller $\alpha\mathcal{P}$, for its communication with the FC. For moderate/high SNR_c, the relative performance of "STC@sensors" and "STC4@sensors" depends on the $\mathcal{P}$ value. Our simulations show that for $\mathcal{P} > 32$ mW, $\alpha\mathcal{P}$ is large enough that "STC4@sensors" provide a larger "decision diversity gain" than that of "STC@sensors" during sensor–FC communication, and thus, the former outperforms the latter. For low SNR_c, however, these schemes have similar performance, since the performance in this regime is limited by the reliability of local decisions at sensors (which are the same for both schemes). Overall, these imply that for wireless sensor networks that

TABLE VI
"PARALLEL," "FUSION@SENSORS," AND "FUSION6@SENSORS," LRT RULE, $\rho = 0$, $\pi_0 = 0.6$, $K = 6$

	$\text{SNR}_c = 10\text{dB}$			$\text{SNR}_c = 6\text{dB}$			$\text{SNR}_c = 2\text{dB}$		
SNR_h	5dB	10dB	15dB	5dB	10dB	15dB	5dB	10dB	15dB
parallel	$3.0e{-3}$	$1.3e{-3}$	$9.0e{-4}$	$3.7e{-2}$	$2.9e{-2}$	$2.7e{-2}$	$1.3e{-1}$	$1.1e{-1}$	$1.1e{-1}$
fusion	$2.8e{-3}$	$8.0e{-4}$	$3.0e{-4}$	$3.5e{-2}$	$2.1e{-2}$	$1.7e{-2}$	$1.2e{-1}$	$9.5e{-2}$	$9.0e{-2}$
fusion6	$3.1e{-3}$	$1.3e{-3}$	$3.1e{-4}$	$3.8e{-2}$	$2.9e{-2}$	$2.6e{-2}$	$1.4e{-1}$	$1.1e{-1}$	$9.9e{-2}$

TABLE VII
ALL SCHEMES, LRT RULE, $\rho = 0$, $\pi_0 = 0.6$, $K = 4$

	$\text{SNR}_c = 10\text{dB}$			$\text{SNR}_c = 6\text{dB}$			$\text{SNR}_c = 2\text{dB}$			
SNR_h	5dB	10dB	15dB	5dB	10dB	15dB	5dB	10dB	15dB	homogenous
parallel	$1.3e{-2}$	$5.9e{-3}$	$5.3e{-3}$	$7.3e{-2}$	$5.8e{-2}$	$5.6e{-2}$	$1.8e{-1}$	$1.5e{-1}$	$1.5e{-1}$	
STC	$2.1e{-2}$	$5.8e{-3}$	$5.1e{-3}$	$8.8e{-2}$	$5.7e{-2}$	$5.4e{-2}$	$1.9e{-1}$	$1.5e{-1}$	$1.5e{-1}$	
fusion	$1.3e{-2}$	$3.8e{-3}$	$3.6e{-3}$	$7.4e{-2}$	$5.2e{-2}$	$4.9e{-2}$	$1.8e{-1}$	$1.5e{-1}$	$1.4e{-1}$	
threshold	$1.5e{-2}$	$2.8e{-3}$	$1.5e{-3}$	$7.8e{-2}$	$4.4e{-2}$	$3.5e{-2}$	$1.7e{-1}$	$1.3e{-1}$	$1.2e{-1}$	
$\mathcal{P}$	3.2mW	10mW	32mW	3.2mW	10mW	32mW	3.2mW	10mW	32mW	inhomogenous
parallel	$1.1e{-2}$	$6.4e{-3}$	$5.2e{-3}$	$7.5e{-2}$	$6.0e{-2}$	$5.8e{-2}$	$1.7e{-1}$	$1.5e{-1}$	$1.5e{-1}$	
STC	$1.4e{-2}$	$6.9e{-3}$	$5.1e{-3}$	$8.4e{-2}$	$5.8e{-2}$	$5.6e{-2}$	$1.8e{-1}$	$1.5e{-1}$	$1.5e{-1}$	
fusion	$1.1e{-2}$	$4.0e{-3}$	$3.6e{-3}$	$7.3e{-2}$	$5.4e{-2}$	$4.9e{-2}$	$1.7e{-1}$	$1.5e{-1}$	$1.4e{-1}$	
threshold	$1.0e{-2}$	$3.6e{-3}$	$1.4e{-3}$	$6.3e{-2}$	$4.5e{-2}$	$3.3e{-2}$	$1.6e{-1}$	$1.4e{-1}$	$1.2e{-1}$	

typically operate within $0.12 \leq \mathcal{P} \leq 36$ mW [27], increasing the number of cooperative partners in a group beyond two does not have much practical incentive. Similarly, going from "fusion@sensors" to "fusion4@sensors," we expect that $(1-\alpha)\mathcal{P}$ increases, whereas $\alpha\mathcal{P}$ decreases. However, different from scheme 1), in scheme 2), local information exchange affects the reliability of local decisions. Hence, the increase in the reliability of the local decisions in "fusion4@sensors" due to the increase of $(1-\alpha)\mathcal{P}$ still compensates for a less reliable sensor–FC communication due to the decrease of $\alpha\mathcal{P}$, which leads to the observation that "fusion4@sensors" outperform "fusion@sensors" for $\mathcal{P} \geq 10$ mW. Going to "fusion6@sensors" for $K = 6$, however, α decreases further, such that even for a large $\mathcal{P} \approx 40$ mW, the unreliability of the sensor–FC communication due to the decrease of $\alpha\mathcal{P}$ leads to the observation that "fusion6@sensors" perform worse than "fusion@sensors" (see Table VI). We expect similar performance degradation as we increase the number of partners in a group beyond six. Going from "threshold changing@sensors" to "threshold changing4@sensors," the former outperforms the latter for all SNR_c and SNR_h. This is due to the fact that as the number of cooperative partners in a group increases, the chance that the corresponding information matrix transmitted by this group to the FC deviates from the conventional orthogonal STC matrix increases, leading to destructive signal interference at the FC and diminishing the "decision diversity gain" of STC. We conjecture similar performance degradation as we increase the number of partners in a group beyond four.

Homogeneous Versus Inhomogeneous Sensor Placement: We consider a network of $K = 4$ sensors, consisting of two groups, where sensors are positioned on the circumference of a circle on the $x-y$ plane, whose center is located at the origin and its diameter is 20 m. The distance between two sensors in each group is $d_0 = 2$ m. For homogeneous placement, we assume that the FC is located at the origin, and for inhomogeneous placement, we move the FC toward one of the groups, such that the distance between the FC and the two groups are 4 and 16 m. Table VII tabulates $\bar{P}_e$ of "parallel," "STC@sensors," "fusion@sensors," and "threshold changing@sensors," as SNR_h and SNR_c vary, for $\pi_0 = 0.6$ and $\rho = 0$, when the FC employs the LRT rule, for homogeneous and inhomogeneous placements. This table shows that our findings on comparison between different schemes are exactly the same as those in Table I, which was another example of a homogenous placement. On the other hand, for inhomogeneous placement, "threshold changing@sensors" outperform other schemes, regardless of $\mathcal{P}$ and SNR_c values. Since "threshold changing@sensors" have the lowest error floor among all schemes, when one group of sensors becomes closer to the FC, the enhanced reliability of the information delivered to the FC by this group leads to the superior performance of this scheme. Comparing "STC@sensors" and "parallel," we note that the former performs worse than the latter in inhomogeneous placement. Since "STC@sensors" and "parallel" have similar error floor, placing one group of sensors closer to the FC does not change the reliability of the information provided by this group to the FC in either schemes. However, since the other group of sensors becomes farther away from the FC, the quality of the information delivered to the FC by this group decreases (due to destructive signal interference of STC), leading to the inferior performance of "STC@sensors."

VIII. CONCLUSION

For the problem of binary distributed detection in a wireless sensor network, we have proposed novel cooperative and parallel fusion architectures, to combat the fading effects encountered in the conventional parallel fusion architecture. In particular, we have proposed 1) cooperative fusion architecture with Alamouti's STC scheme at sensors, 2) cooperative fusion architecture with signal fusion at sensors, and 3) parallel fusion architecture with local threshold changing at sensors. While there is limited local information exchange among the sensors (1-bit message) in schemes 1) and 2), there is no explicit information exchange in scheme 3). For these schemes, we derived the optimal LRT and the suboptimal majority fusion rules and analyzed their performance, in terms of communication and sensing SNRs. Our numerical results show that when the FC employs the LRT rule, unless for low communication SNR and moderate/high sensing SNR, performance improvement is feasible with the new cooperative and parallel fusion architectures, while scheme 3) outperforms the others. When the FC utilizes the majority rule, such improvement is possible, unless for high sensing SNR. In particular, for very high sensing SNR, scheme 1) outperforms the others, whereas for moderate/low sensing SNR, scheme 2) outperforms the others.

APPENDIX

Upper Bounds on $\mathcal{T}_{e_1|h}$ in (23) and its average $\bar{\mathcal{T}}_{e_1}$: For $Q_n < M$, we have

$$\mathcal{T}_{e_1|h} = P\left(\sum_{d_{n_1,m_1}\in S_1} d_{n_1,m_1} > -\sum_{d_{n_1,m_1}\in S_0} d_{n_1,m_1}|F_{n,m}\right) < P\left(\sum_{d_{n_1,m_1}\in S_1} d_{n_1,m_1} > -d_{n,m}|F_{n,m}\right) \quad (48)$$

where the bound in (48) is obtained, noting that $d_{n,m} \in S_0$ and that $\sum_{d_{n_1,m_1}\in S_0} d_{n_1,m_1} < d_{n,m}$. To further bound (48), we define interval x and function φ, as follows:

$$x = \mathbb{E}\left\{\sum_{d_{n_1,m_1}\in S_1} C_{n_1,m_1} d_{n_1,m_1}|F_{n,m}\right\}$$

$$\varphi(x) = P\left(\sum_{d_{n_1,m_1}\in S_1} C_{n_1,m_1} d_{n_1,m_1} > -d_{n,m}|F_{n,m}\right) \quad (49)$$

where constants C_{n_1,m_1} take values in the interval $[0, |S_1|]$. Our numerical results suggest that for small $|S_1|$, φ is convex over x. Invoking the inequality $\varphi(\sum_{i=1}^n x_i/n) \leq (\sum_{i=1}^n \varphi(x_i)/n)$, where the points $x_1, \ldots, x_n$ belong to x [26], and letting $n = |S_1|$ and $x_i = \mathbb{E}\{|S_1|d_{n_1,m_1}|F_{n,m}\}$ for $i = 1, \ldots, |S_1|$, we establish the following:

$$\varphi\left(\sum_{d_{n_1,m_1}\in S_1} \mathbb{E}\{d_{n_1,m_1}|F_{n,m}\}\right) = \varphi\left(\frac{1}{|S_1|}\sum_{d_{n_1,m_1}\in S_1} \mathbb{E}\left\{|S_1|d_{n_1,m_1}|F_{n,m}\right\}\right) \leq \frac{1}{|S_1|}\sum_{d_{n_1,m_1}\in S_1} \varphi\left(\mathbb{E}\left\{|S_1|d_{n_1,m_1}|F_{n,m}\right\}\right). \quad (50)$$

The inequality in (50) implies that the upper bound on $\mathcal{T}_{e_1|h}$ in (48) can be further bounded as

$$P\left(\sum_{d_{n_1,m_1}\in S_1} d_{n_1,m_1} > -d_{n,m}|F_{n,m}\right) \leq \frac{1}{|S_1|}\sum_{d_{n_1,m_1}\in S_1} P\left(|S_1|d_{n_1,m_1} > -d_{n,m}|F_{n,m}\right). \quad (51)$$

The new bound on $\mathcal{T}_{e_1|h}$ in (51) can be presented in closed form, considering the definitions of $d_{n,m}$ and d_{n_1,m_1} in (21) and noting that, conditioned on $u_{2s-1}, u_{2s}, \hat{u}_{2s-1}, \hat{u}_{2s}$, the terms z_{2s-1}, z_{2s} are independent complex Gaussian RVs with the variance $\sigma^2 = (|h_{2s-1}|^2 + |h_{2s}|^2)\sigma_v^2$ and the mean values $\mu_{2s-1}^{n_1,m_1}, \mu_{2s}^{n_1,m_1}$ for d_{n_1,m_1} and $\mu_{2s-1}^{n,m}, \mu_{2s}^{n,m}$ for $d_{n,m}$. Mapping the noise terms $\delta_{ij}^1, \delta_{ij}^2$ in Section III-B into δ_s^1, δ_s^2, we find

$$P\left(|S_1|d_{n_1,m_1} > -d_{n,m}|F_{n,m}\right) = P\left(\zeta(n,m,n_1,m_1) > -\ln\left(|S_1|G(n,m,n_1,m_1)\right) + I(n,m,n_1,m_1)\right) \quad (52)$$

where $G(n,m,n_1,m_1)$ is defined in (27), and $I(n,m,n_1,m_1) = \sum_{s=1}^S \mathcal{K}_s(n,m,n_1,m_1)$ in which

$$\begin{aligned}\mathcal{K}_s(n,m,n_1,m_1) &= \frac{1}{\sigma^2}\left(\left|\mu_{2s-1}^{n_1,m_1} - \mu_{2s-1}^{n,m}\right|^2 + \left|\mu_{2s}^{n_1,m_1} - \mu_{2s}^{n,m}\right|^2\right)\\ &= \frac{\alpha}{2\sigma_v^2}\left(\left|h_{2s-1}(a_{n_1}^{2s-1} - a_n^{2s-1}) + h_{2s}\left(a_{n_1}^{2s} - a_n^{2s}\right)\right|^2 + \left|h_{2s-1}\left(a_{m_1}^{2s-1} - a_m^{2s-1}\right) + h_{2s}\left(a_{m_1}^{2s} - a_m^{2s}\right)\right|^2\right)\end{aligned} \quad (53)$$

$$\zeta(n,m,n_1,m_1) = \sum_{s=1}^S \theta_s(n,m,n_1,m_1) \quad \text{where} \quad \theta_s(n,m,n_1,m_1) = \frac{2}{\sigma^2}\mathfrak{Re}\left\{\delta_s^1\left(\mu_{2s-1}^{n_1,m_1} - \mu_{2s-1}^{n,m}\right)^* + \delta_s^2\left(\mu_{2s}^{n_1,m_1} - \mu_{2s}^{n,m}\right)^*\right\}. \quad (54)$$

Recall that δ_s^1 and δ_s^2 are i.i.d. zero-mean complex Gaussian RVs with variance σ^2. Hence, $\zeta(n,m,n_1,m_1)$ is a zero-mean Gaussian RV with variance $2I(n,m,n_1,m_1)$. Thus, we can express (52) as

$$P\left(|S_1|d_{n_1,m_1} > -d_{n,m}|F_{n,m}\right) = Q\left(\frac{-\ln\left(|S_1|G(n,m,n_1,m_1)\right) + I(n,m,n_1,m_1)}{\sqrt{2I(n,m,n_1,m_1)}}\right). \quad (55)$$

Note that $I(n,m,n_1,m_1)$ depends on the coefficients h_{2s-1}, h_{2s}, whereas $G(n,m,n_1,m_1)$ is independent of these coefficients. In fact, $G(n,m,n_1,m_1)$ depends on sensing channels through P_d, P_f and the average received SNR $\bar{\gamma}_{hs}$ corresponding to internode communication through $T_{n,m}, T_{n_1,m_1}$. One can verify that when $\pi_0 > \pi_1$, we have $-\ln(|S_1|G(n,m,n_1,m_1)) + I(n,m,n_1,m_1) > 0$. Combining (48), (51), and (55), using the Chernoff bound of Q-function $Q(x) < (1/2)e^{-(x^2/2)}$ for $x > 0$ and noting that $0 < e^{(-(\ln(|S_1|G(n,m,n_1,m_1)))^2/4I(n,m,n_1,m_1))} < 1$ and, thus, can be dropped without decreasing the upper bound, we find

$$\mathcal{T}_{e_1|h} < \frac{\mathbf{1}_{\{Q_n<M\}}}{2\sqrt{|S_1|}}\sum_{d_{n_1,m_1}\in S_1}\sqrt{G(n,m,n_1,m_1)} \times e^{-\frac{I(n,m,n_1,m_1)}{4}} + \mathbf{1}_{\{Q_n\geq M\}}. \quad (56)$$

Finally, to find an upper bound on $\bar{\mathcal{T}}_{e_1}$, we need to take the average of $e^{-(I(n,m,n_1,m_1)/4)}$ in (56) over h_{2s-1}, h_{2s} for $s = 1,\ldots,S$. Since $h_{2s-1}, h_{2s} \sim \mathcal{CN}(0,\sigma_h^2)$ are i.i.d. across the pairs, we have

$$\mathbb{E}\left\{e^{-\frac{I(n,m,n_1,m_1)}{4}}\right\} = \prod_{s=1}^{S} \int_{h_{2s-1}} \int_{h_{2s}} e^{\frac{-\mathcal{K}_s(n,m,n_1,m_1)}{4}} e^{-\frac{\left(|h_{2s-1}|^2+|h_{2s}|^2\right)}{\sigma_h^2}} d_{h_{2s-1}} d_{h_{2s}}. \tag{57}$$

After some calculations, (57) is reduced to $\prod_{s=1}^{S} \mathcal{D}_1(n,m,n_1,m_1)$, where $\mathcal{D}_1(n,m,n_1,m_1)$ is given in (28). The upper bound on $\bar{\mathcal{T}}_{e_1}$ is obtained by substituting $e^{-(I(n,m,n_1,m_1)/4)}$ in (56) with $\prod_{s=1}^{S} \mathcal{D}_1(n,m,n_1,m_1)$. This completes our derivations for the upper bound on $\bar{\mathcal{T}}_{e_1}$.

Upper Bounds on $\mathcal{T}_{e_2|h}$ in (24) and its average $\bar{\mathcal{T}}_{e_2}$: For $Q_n > M$, we have

$$\mathcal{T}_{e_2|h} < P(d_{n,m} < -\sum_{d_{n_1,m_1}\in S_0} d_{n_1,m_1}|F_{n,m}) < \frac{1}{|S_0|} \sum_{d_{n_1,m_1}\in S_0} P(d_{n,m} < -|S_0| d_{n_1,m_1}|F_{n,m}) \tag{58}$$

noting that $d_{n,m} \in S_1$ and $\sum_{d_{n_1,m_1}\in S_1} d_{n_1,m_1} > d_{n,m}$. The new bound on $\mathcal{T}_{e_2|h}$ in (58) can be found in closed form, via examining the definitions of $d_{n,m}$ and d_{n_1,m_1} in (21) and noting that, conditioned on $u_{2s-1}, u_{2s}, \hat{u}_{2s-1}, \hat{u}_{2s}$, the terms z_{2s-1}, z_{2s} are independent complex Gaussian RVs with variance $\sigma^2 = (|h_{2s-1}|^2 + |h_{2s}|^2)\sigma_v^2$ and mean values $\mu_{2s-1}^{n_1,m_1}, \mu_{2s}^{n_1,m_1}$ for d_{n_1,m_1} and $\mu_{2s-1}^{n,m}, \mu_{2s}^{n,m}$ for $d_{n,m}$. Therefore

$$P\left(d_{n,m} < -|S_0| d_{n_1,m_1}|F_{n,m}\right) = P\left(\zeta(n,m,n_1,m_1) > -\ln\left(|S_0| G(n,m,n_1,m_1)\right) + I(n,m,n_1,m_1)\right). \tag{59}$$

Comparing (52) and (59), it seems natural to write (59) in terms of the Q-function and apply the Chernoff bound to reach a bound. However, different from (52), when $\pi_0 > \pi_1$, we no longer have $-\ln(|S_0|G(n,m,n_1,m_1)) + I(n,m,n_1,m_1) > 0$. We use an alternative bound, which states $P(\sum_{s=1}^{S} x_s < a) < \min_{t,t>0} e^{ta} \prod_{s=1}^{S} \mathbb{E}\{e^{-tx_s}\}$ when $x_1,\ldots,x_S$ are independent RVs [26]. Combining (58) and (59), letting $x_s = -\theta_s(n,m,n_1,m_1)$, $a = \ln(|S_0|G(n,m,n_1,m_1)) - I(n,m,n_1,m_1)$ in (59), and using the alternative bound, we find

$$\mathcal{T}_{e_2|h} < \frac{\mathbf{1}_{\{Q_n>M\}}}{|S_0|} \sum_{d_{n_1,m_1}\in S_0} \left[\min_t e^{-tI(n,m,n_1,m_1)} \times \left(|S_0| G(n,m,n_1,m_1)\right)^t \prod_{s=1}^{S} \mathbb{E}\left\{e^{t\theta_s(n,m,n_1,m_1)}\right\}\right] + \mathbf{1}_{\{Q_n\le M\}}. \tag{60}$$

Noting that $-\theta_s(n,m,n_1,m_1) \sim \mathcal{CN}(0, 2\mathcal{K}_s(n,m,n_1,m_1))$ and using the moment-generating function results, we find $\mathbb{E}\{e^{t\theta_s(n,m,n_1,m_1)}\} = e^{t^2\mathcal{K}_s(n,m,n_1,m_1)}$. This implies that we can rewrite (60) as follows:

$$\mathcal{T}_{e_2|h} < \frac{\mathbf{1}_{\{Q_n>M\}}}{|S_0|} \sum_{d_{n_1,m_1}\in S_0} \left[\min_t (|S_0|G(n,m,n_1,m_1))^t \times \prod_{s=1}^{S} e^{(t^2-t)\mathcal{K}_s(n,m,n_1,m_1)}\right] + \mathbf{1}_{\{Q_n\le M\}}. \tag{61}$$

To find a bound on $\bar{\mathcal{T}}_{e_2}$, we need to take the average of $e^{(t^2-t)\mathcal{K}_s(n,m,n_1,m_1)}$ in (61) over h_{2s-1}, h_{2s}. One can verify that this term is equal to $\mathcal{D}_2(n,m,n_1,m_1)$ in (29). The upper bound on $\bar{\mathcal{T}}_{e_2}$ is obtained by substituting $e^{(t^2-t)\mathcal{K}_s(n,m,n_1,m_1)}$ in (61) with (29). This completes our derivations for the bound on $\bar{\mathcal{T}}_{e_2}$.

References

[1] B. Chen, R. Jiang, T. Kasetkasem, and P. K. Varshney, "Channel aware decision fusion in wireless sensor networks," *IEEE Trans. Signal Process.*, vol. 52, no. 12, pp. 3454–3458, Dec. 2004.

[2] R. Niu, B. Chen, and P. K. Varshney, "Fusion of decisions transmitted over Rayleigh fading channels in wireless sensor networks," *IEEE Trans. Signal Process.*, vol. 54, no. 3, pp. 1018–1027, Mar. 2006.

[3] B. Chen, L. Tong, and P. K. Varshney, "Channel-aware distributed detection in wireless sensor networks," *IEEE Signal Process. Mag.*, vol. 23, no. 4, pp. 16–26, Jul. 2006.

[4] R. Jiang, S. Misra, B. Chen, and A. Swami, "Robust suboptimal decision fusion in wireless sensor networks," in *IEEE Proc. MILCOM*, Oct. 2005, pp. 2107–2113.

[5] H. Kim, J. Wang, P. Cai, and S. Cui, "Detection outage and detection diversity in a homogeneous distributed sensor network," *IEEE Trans. Signal Process.*, vol. 57, no. 7, pp. 2875–2881, Jul. 2009.

[6] K. Lai, Y. Yang, and J. Jia, "Fusion of decisions transmitted over flat fading channels via maximizing the deflection coefficient," *IEEE Trans. Veh. Technol.*, vol. 59, no. 7, pp. 3634–3640, Sep. 2010.

[7] J. Chamberland and V. V. Veeravalli, "Asymptotic results for decentralized detection in power constrained wireless sensor networks," *IEEE J. Sel. Areas Commun.*, vol. 22, no. 6, pp. 1007–1015, Aug. 2004.

[8] J. Chamberland and V. V. Veeravalli, "The impact of fading on decentralized detection in power constrained wireless sensor networks," in *Proc. IEEE ICASSP*, May 2004, pp. 837–840.

[9] B. Chen and P. K. Willet, "On the optimality of the likelihood-ratio test for local sensor decision rules in the presence of nonideal channel," *IEEE Trans. Inf. Theory*, vol. 51, no. 2, pp. 693–699, Feb. 2005.

[10] V. R. Kanchumarthy, R. Viswanathan, and M. Madishetty, "Impact of channel errors on decentralized detection performance of wireless sensor networks: A study of binary modulations, Rayleigh-fading and nonfading channels, and fusion-combiners," *IEEE Trans. Signal Process.*, vol. 56, no. 5, pp. 1761–1769, May 2008.

[11] R. Jiang and B. Chen, "Fusion of censored decisions in wireless sensor networks," *IEEE Trans. Wireless Commun.*, vol. 4, no. 6, pp. 2668–2673, Nov. 2005.

[12] A. Lei and R. Schober, "Multiple-symbol differential decision fusion for mobile wireless sensor networks," *IEEE Trans. Wireless Commun.*, vol. 9, no. 2, pp. 778–790, Feb. 2010.

[13] J. N. Laneman, D. N. C. Tse, and G. W. Wornell, "Cooperative diversity in wireless networks: Efficient protocols and outage behavior," *IEEE Trans. Inf. Theory*, vol. 50, no. 12, pp. 3062–3080, Dec. 2004.

[14] P. F. Swaszek and P. Willett, "Parley as an approach to distributed detection," *IEEE Trans. Aerosp. Electron. Syst.*, vol. 31, no. 1, pp. 447–457, Jan. 1995.

[15] D. Pados, K. W. Halford, D. Kazakos, and P. Papantoni-Kazakos, "Distributed binary hypothesis testing with feedback," *IEEE Trans. Syst., Man, Cybern.*, vol. 25, no. 1, pp. 21–42, Jan. 1995.

[16] Y. W. Hong, A. Scaglione, and P. K. Varshney, "A communication architecture for reaching consensus in decision for a large network," in *Proc. IEEE Workshop SSP*, 2005, pp. 1220–1225.

[17] P. Braca, S. Marano, V. Matta, and P. Willett, "Asymptotic optimality of running consensus in testing binary hypotheses," *IEEE Trans. Signal Process.*, vol. 58, no. 2, pp. 814–825, Feb. 2010.

[18] Y. Jia and A. Vosoughi, "Impact of channel estimation error upon sum-rate in amplify-and-forward two-way relaying systems," in *Proc. IEEE Workshop SPAWC*, 2010, pp. 1–5.
[19] H. Ahmadi and A. Vosoughi, "Space–time coding for distributed detection in wireless sensor networks," in *Proc. IEEE Workshop SPAWC*, 2009, pp. 329–333.
[20] S. M. Alamouti, "A simple transmit diversity technique for wireless communications," *IEEE J. Sel. Areas Commun.*, vol. 16, no. 8, pp. 1451–1458, Oct. 1998.
[21] W. Zhang and K. B. Letaief, "Cooperative spectrum sensing with transmit and relay diversity in cognitive radio networks," *IEEE Trans. Wireless Comm.*, vol. 7, no. 12, pp. 4761–4766, Dec. 2008.
[22] N. Katenka, E. Levina, and G. Michailidis, "Local vote decision fusion for target detection in wireless sensor networks," *IEEE Trans. Signal Process.*, vol. 56, no. 1, pp. 329–338, Jan. 2008.
[23] W. P. Tay, "The value of feedback in decentralized detection," *IEEE Trans. Inf. Theory*, vol. 58, no. 1, pp. 7226–7239, Dec. 2012.
[24] O. P. Kreidl, J. N. Tsitsiklis, and S. I. Zoumpoulis, "On decentralized detection with partial information sharing among sensors," *IEEE Trans. Signal Process.*, vol. 59, no. 4, pp. 1759–765, Apr. 2011.
[25] H. Shalaby and A. Papamarcou, "A note on the asymptotics of distributed detection with feedback," *IEEE Trans. Inf. Theory*, vol. 39, no. 2, pp. 633–640, Mar. 1993.
[26] S. Boyd and L. Vandenberghe, *Convex Optimization*. Cambridge, U.K.: Cambridge Univ. Press, 2004.
[27] V. Raghunathan, C. Schurgers, S. Park, and M. B. Srivastava, "Energy-aware wireless microsensor networks," *IEEE Signal Process. Mag.*, vol. 10, no. 2, pp. 40–50, Mar. 2002.
[28] [Online]. Available: http://arxiv.org/abs/1508.07913v3

Nahal Maleki (S'15) received the B.S. degree in electrical engineering (electronics) from Shiraz University, Shiraz, Iran, in 2001 and the M.S. degree in electrical engineering (communication) from the University of Tehran, Tehran, Iran, in 2004. She is currently working toward the Ph.D. degree in electrical engineering (communications) with the Department of Electrical and Computer Engineering, University of Rochester, Rochester, NY, USA.

Her research interests include wireless of wireless communication systems, specifically in the capacity enhancement methods for code-division multiple-access cellular systems, wireless communications, statistical signal processing, distributed detection, and estimation theory.

Azadeh Vosoughi (M'06–SM'14) received the B.S. degree from Sharif University of Technology, Tehran, Iran, in 1997; the M.S. degree from Worcester Polytechnic Institute, Worcester, MA, USA, in 2001; and the Ph.D. degree from Cornell University, Ithaca, NY, USA, in 2006, all in electrical engineering.

She is an Associate Professor with the Department of Electrical Engineering and Computer Science, University of Central Florida, Orlando, FL, USA. Her research interests include wireless communications, statistical signal processing, distributed detection and estimation theory, and brain signal processing.

Dr. Vosoughi received the National Science Foundation CAREER Award in 2011. She is currently serving as an Associate Editor for the IEEE SIGNAL PROCESSING LETTERS.

Nazanin Rahnavard (S'97–M'10) received the B.S. and M.S. degrees in electrical engineering from Sharif University of Technology, Tehran, Iran, in 1999 and 2001, respectively, and the Ph.D. degree from the School of Electrical and Computer Engineering, Georgia Institute of Technology (Georgia Tech), Atlanta, GA, USA, in 2007.

She is currently an Associate Professor with the Department of Electrical Engineering and Computer Science, University of Central Florida, Orlando, FL, USA. She has interest and expertise in a variety of research topics in the areas of communications, networking, and signal processing.

Dr. Rahnavard received the National Science Foundation CAREER Award in 2011. She also received the 2007 Outstanding Research Award from the Center of Signal and Image Processing, Georgia Tech. She serves on the Editorial Board of Elsevier's *Journal on Computer Networks* (COMNET) and on the Technical Program Committee of several prestigious international conferences.